BIC9127359

CNEN/SP

ipen *Instituto de Pesquisas Energéticas e Nucleares*

GVTRAN—PC — A STEAM GENERATOR TRANSIENT SIMULATOR

Horácio NAKATA

iPEN, PUB -- 329.

SÃO PAULO

GVTRAN—PC - A   STEAM   GENERATOR   TRANSIENT   SIMULATOR

Horácio NAKATA

DEPARTAMENTO DE TECNOLOGIA DE REATORES

INIS Categories and Descriptors

E32.00
F51.00

STEAM GENERATORS
COMPUTERIZED SIMULATION

GVTRAN–PC – A STEAM GENERATOR TRANSIENT SIMULATOR

Horácio NAKATA

COMISSÃO NACIONAL DE ENERGIA NUCLEAR – SP
INSTITUTO DE PESQUISAS ENERGÉTICAS E NUCLEARES
Caixa Postal 11049 – Pinheiros
05499 – São Paulo–SP – BRASIL

ABSTRACT

Since an accurate and inexpensive analysis capability is one of the desirable requirement in the reactor licensing procedure and, also, in instances when a severe accident sequence and its degree of severity must be estimated, the present work tries partially to fulfill that present need by developing a fast and acceptably accurate simulator. The present report presents the methodology utilized to develop GVTRAN–PC program, the steam generator simulation program for the microcomputer environment, which possess a capability to reproduce the experimental data with accuracies comparable to those of the mainframe simulators. The methodology is based on the mass and energy conservation in the control volumes which represents both the primary and the secondary fluid in the U–tube steam generator. The quasi–static momentum conservation in the secondary fluid control volumes determines in a semi–iterative scheme the liquid level in the feedwater chamber. The implementation of the moving boundary technique has allowed the tracking of the boundary of bulk boiling region with the utilization of a reduced number of control volumes in the tube region. GVTRAN–PC program has been tested against typical PWR pump trip transient experimental data and the calculation results showed good agreement in most representative parameters, viz. the feedchamber water–level and the steam dome pressure.

GVTRAN-PC – SIMULADOR DE GERADOR DE VAPOR

Horácio NAKATA

COMISSÃO NACIONAL DE ENERGIA NUCLEAR – SP
INSTITUTO DE PESQUISAS ENERGÉTICAS E NUCLEARES
Caixa Postal 11049 – Pinheiros
05499 – São Paulo—SP – BRASIL

RESUMO

O presente trabalho apresenta a metodologia desenvolvida para a construção do programa GVTRAN-PC, um simulador para análise de performance de gerador de vapor de uma planta nuclear. A metodologia é baseada na conservação de massa e energia tanto no circuito primário como no circuito secundário do gerador de vapor. Aproximação quase—estática na conservação de momento no circuito secundário determina de maneira semi—iterativa o nível de líquido na câmara de admissão de água. O programa faz uso da técnica de fronteira móvel para a representação da altura da região de ebulição saturada, permitindo a utilização de reduzido número de volumes de controle na região dos tubos, reproduzindo porém os resultados experimentais com precisão comparável a dos programas simuladores de grande porte. O programa GVTRAN-PC foi testado contra resultados experimentais de uma parada de bomba em uma planta nuclear típica, e os resultados calculados mostraram boa concordância nos parâmetros mais representativos, por ex no nível de água na câmara de admissão e na pressão do vapor.

1. INTRODUCTION

An accurate and inexpensive analysis capability is one of the upmost desirable quality which is sought in a plant simulator, for the licensing procedure and operation managements require a great number of detailed plant performance evaluations under hypothetical accident sequences and initiating conditions. Nevertheless, in view of the increasing analytical complexity, the existing codes are not fast enough to permit thoroughly examination of all the most probable sequences in an accident analysis. The present work tries to contribute to the development of a faster and better plant simulator, by developing a fast and accurate microcomputer based steam generator simulator.

The present report presents the methodology developed and implemented in GVTRAN–PC program, the steam generator simulator for the microcomputer environment. The primary circuit of the steam generator is simply treated with the mass and energy conservation equations, by assuming a constant pressure in the primary tube region. In the secondary circuit the mass and energy conservation are imposed with properly chosen two–phase correlations. The feedchamber water level are determined with the momentum conservation equation in a quasi–static approximation.

The simplicity of GVTRAN–PC program is also warranted by a reduced number of control volumes both in the primary and in the secondary region. The most important effect in the secondary region which must be carefully tracked is the level at which the bulk boiling initiates because the void fraction changes quite abruptly at that point and, consequently, strongly influencing the heat transfer rate from the primary to the secondary fluid. The program tracks the boundary of bulk boiling region with the moving boundary approach by defining only two control volumes in the secondary tube zone and, correspondingly, four control volumes in the primary tube zone.

The performance of GVTRAN–PC program has been evaluated by calculating a pump trip transient recorded during a startup testing of Donald C. Cook Nuclear Station Unit One. The calculated results were favorably compared with the experimental data and the quality of the results is satisfactory even in comparison to the four–equation non–equilibrium liquid model implemented in the main frame steam generator TRANSG simulator.

In overall, GVTRAN–PC program possess a set of qualities which highly commends for its implementation in a nuclear plant simulator, vis. coding simplicity, computation velocity and acceptable accuracy.

2. METHODOLOGY

GVTRAN program solves the equations for the mass, energy and momentum conservation in the secondary side of the steam generator, while in the primary side only mass and energy conservations are specified and a constant pressure assumption is considered. The conservation equations are solved numerically with the Classical Runge–Kutta method with the suitable mesh spacings for stability requirements. In the following paragraphs the detailed descriptions of the methodology are presented.

2.1 Conservation Equations in the Control Volume

The conservation equations for the steam generator modelling are listed below. The terms related to the kinetic energy, potential energy and viscous heat dissipation will be neglected.

The laws of conservation for an infinitesimal volume element are for the mass conservation equation

$$\frac{\partial}{\partial t}\rho = -\nabla\cdot(\rho\,\vec{v}) ,\tag{2.1.1}$$

for the momentum conservation equation

$$\frac{\partial}{\partial t}(\rho\vec{v}) = -\nabla\cdot(\rho\underline{v}\,\underline{v}) - \nabla\cdot\underline{\tau} - \nabla\cdot\underline{P} + \rho\vec{g}\tag{2.1.2}$$

and for the energy conservation equation

$$\frac{\partial}{\partial t}(\rho h) = -\nabla\cdot(\rho h\vec{v}) - \nabla\cdot\vec{q} + \frac{\partial}{\partial t}P ,\tag{2.1.3}$$

where conventional notations are used, such as

ρ	= fluid density,
$\vec{v}$	= fluid velocity,
$\vec{g}$	= acceleration of gravity,
h	= fluid enthalpy,
P	= pressure,
$\underline{v}\,\underline{v}$	= velocity tensor,
$\underline{\tau}$	= shear stress tensor,
$\underline{P}$	= normal pressure tensor, and
$\vec{q}$	= heat flux.

In general the control volumes outer surfaces are nonstationary, that is, there can be a moving boundary between adjacent control volumes. The Leibnits's integration rule is therefore used for the macroscopic balances

$$\frac{d}{dt}\int_{V(t)} \phi \, dV = \int_{V(t)} \frac{\partial}{\partial t}\phi \, dV + \oint_{V_o(t)} \phi \vec{v}_o \cdot d\vec{s} \qquad (2.1.4)$$

where

ϕ is the variable to be balanced in the control volume $V(t)$,

$V_o(t)$ is the control volume surface,

$\vec{v}_o$ is the velocity of the surface $V_o(t)$,
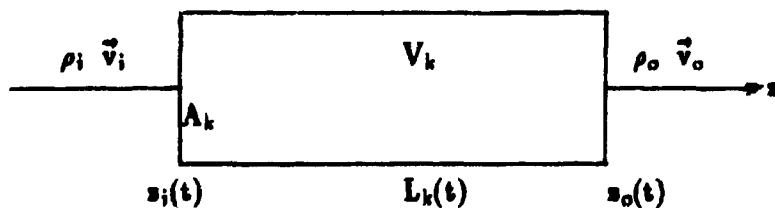
$\vec{s}$ is the normal area.

In the one-dimensional geometry the Leibnits's rule is written as

$$\frac{d}{dt}\int_{a(t)}^{b(t)} \phi \, ds = \int_{a(t)}^{b(t)} \frac{\partial}{\partial t}\phi \, ds + \phi(b)\frac{d}{dt}b(t) - \phi(a)\frac{d}{dt}a(t) \qquad (2.1.5)$$

2.2   Macroscopic Mass Conservation

The figure below illustrates the one-dimensional control volume model implemented in the program.

Constant flow area A_k is assumed, such that Equation 2.1.1. becomes

$$\frac{\partial}{\partial t}\rho = -\frac{d}{ds}(\rho v). \qquad (2.2.1)$$

Integrating Equation 2.2.1 in the volume V_k, one gets

$$A_k \int_{s_i(t)}^{s_o(t)} \frac{\partial}{\partial t}\rho\, ds = - A_k \int_{s_i(t)}^{s_o(t)} \frac{d}{ds}(\rho v)\, ds. \qquad (2.2.2)$$

Expansion of the left hand side of Equation 2.2.2 gives, with the Leibnitz's rule,

$$A_k \int_{s_i(t)}^{s_o(t)} \frac{\partial}{\partial t}\rho\, ds = - A_k \frac{d}{dt} \int_{s_i(t)}^{s_o(t)} \rho\, ds - A_k \rho_o v_{so} + A_k \rho_i v_{si}$$

$$= - A_k \frac{d}{dt}(\bar{\rho}_k L_k) - A_k \rho_o v_{so} + A_k \rho_i v_{si}$$

$$(2.2.3)$$

where

$$\bar{\rho}_k = \int_{s_i(t)}^{s_o(t)} \rho\, ds / L_k \quad \text{is the average density in the control volume } V_k,$$

v_{si}, v_{so} are the velocities of the left and right boundaries of the control volume V_k, respectively.

Substitution of Equation 2.2.3 in Equation 2.2.2 followed by integration of the right hand side terms results in

$$\frac{d}{dt}(\bar{\rho}_k A_k L_k) - A_k \rho_o v_{so} + A_k \rho_i v_{si} = A_k \rho_i v_i + A_k \rho_o v_o$$

or rearranging the terms

$$\frac{d}{dt}(\bar{\rho}_k A_k L_k) = A_k \rho_i(v_i - v_{si}) - A_k \rho_o(v_o - v_{so}). \qquad (2.2.4)$$

The right hand side of Equation 2.2.4 represents mass inflow and mass outflow in the control volume V_k,

$$W_i = A_k \rho_i(v_i - v_{si}) \qquad (2.2.5)$$

and

$$W_o = A_k \rho_o(v_o - v_{so}), \qquad (2.2.6)$$

such that the mass conservation equation, Equation 2.2.4, can be rewritten as

$$\frac{d}{dt}(\bar{\rho}_k A_k L_k) = W_i - W_o \tag{2.2.7}$$

or

$$\frac{d}{dt}\bar{\rho}_k = \frac{W_i - W_o - \bar{\rho}_k A_k \frac{d}{dt} L_k}{A_k L_k} \tag{2.2.8}$$

2.3 Macroscopic Momentum Conservation

The momentum conservation equation, Equation 2.1.2, is integrated in the control volume V_k,

$$\int \frac{\partial}{\partial t}(\rho\vec{v})dV = -\int \nabla\cdot(\rho\underline{v}\,\underline{v})dV - \int \nabla\cdot\underline{\tau}dV - \int \nabla\cdot\underline{P}dV + \int \rho\vec{g}dV \tag{2.3.1}$$

With the Leibnitz's rule the left hand side becomes

$$\int_V \frac{\partial}{\partial t}(\rho v)dV = \frac{d}{dt}G_k(t) - A_k\rho_o v_o v_{so} + A_k\rho_i v_i v_{si} \tag{2.3.2}$$

where

$$G_k(t) = A_k\int_{s_i(t)}^{s_o(t)}(\rho v)ds. \tag{2.3.3}$$

The first term on the right hand side can be simplified, in one-dimensional geometry, as

$$-\int_V \nabla\cdot(\rho\underline{v}\,\underline{v})dV = -A_k\int_{s_i(t)}^{s_o(t)}\frac{\partial}{\partial s}(\rho v^2)\,ds \tag{2.3.4}$$

or

$$-\int_V \nabla \cdot (\rho \underline{v} \, \underline{v}) dV = -A_k \rho_o v_o^2 + A_k \rho_i v_i^2 . \qquad (2.3.5)$$

With divergence theorem, the second term on the right hand side of Equation 2.3.1 becomes

$$-\int_V \nabla \cdot \underline{\tau} \, dV = -\oint_{V_s} \underline{\underline{\tau}} \, d\vec{s} .$$

Assuming only viscous forces parallel to the walls and defining the friction factor(Fanning), f_p, as

$$f_p = \frac{\tau_w}{1/2(\rho v^2)} ,$$

one obtains

$$-\int_V \nabla \cdot \underline{\tau} \, dV = -A_k \int_{s_i(t)}^{s_o(t)} \frac{2\rho v^2}{D_e} f_p ds \qquad (2.3.6)$$

where D_e is the equivalent hydraulic diameter.

Assuming constant friction factor f_p along the control volume, and also an average value for the momentum in control volume, one gets from Equation 2.3.6

$$-\int_V \nabla \cdot \underline{\tau} \, dV = -A_k L_k \frac{2\rho v^2}{D_e} f_p . \qquad (2.3.7)$$

The third term on the right hand side of Equation 2.3.1, for one-dimensional geometry, can be simplified as

$$-\int_V \nabla \cdot \underline{P} \, dV = -\oint_{V_s} \underline{P} \, d\vec{s} = -A_k P_o + A_k P_i. \qquad (2.3.8)$$

The last term of the right hand side of Equation 2.3.1 becomes

$$\int_V \rho \vec{g} dV = A_k g \cos\theta (\rho_o s_o - \rho_i s_i) \qquad (2.3.9)$$

where θ is the angle between s direction and the gravity force.

With the substitution of Equation 2.3.2, 2.3.5, 2.3.7, 2.3.8 and 2.3.9 in Equation 2.3.1, one gets

$$\frac{d}{dt}G_k(t) = A_k\rho_i v_i(v_i - v_{si}) - A_k\rho_o v_o(v_o - v_{so}) - A_k L_k \frac{2\rho v^2}{D_e} f_F$$

$$A_k P_i - A_k P_o + A_k g \cos\theta(\rho_o s_o - \rho_i s_i). \tag{2.3.10}$$

Recalling the mass flow definitions, Equation 2.2.5 and 2.2.6, Equation 2.3.10 can be rewritten as

$$\frac{d}{dt}G_k(t) = W_i v_i - W_o v_o - A_k L_k \frac{2\rho v^2}{D_e} f_F$$

$$A_k P_i - A_k P_o + A_k g \cos\theta(\rho_o s_o - \rho_i s_i). \tag{2.3.11}$$

2.4   Macroscopic Energy Conservation

The energy conservation, Equation 2.1.3, is integrated in the control volume yielding

$$\int \frac{\partial}{\partial t}(\rho h)dV = -\int \nabla\cdot(\rho h\vec{v})dV - \int \nabla\cdot\vec{q}dV + \int \frac{\partial}{\partial t}PdV. \tag{2.4.1}$$

The left hand side of Equation 2.4.2 can be rewritten, with the Leibnits's rule, as

$$\int_V \frac{\partial}{\partial t}(\rho h)dV = \frac{d}{dt}\int_V (\rho h)dV - A_k\rho_o h_o v_{so} + A_k\rho_i h_i v_{si}. \tag{2.4.2}$$

The first term on the right hand side of Equation 2.4.1 becomes, with the divergence theorem,

$$-\int \nabla\cdot(\rho h\vec{v})dV = -A_k\rho_o h_o v_o + A_k\rho_i h_i v_i . \tag{2.4.3}$$

12

The second term on the right hand side of Equation 2.4.1 becomes

$$-\int_V \vec{\nabla} \cdot \vec{q} dV = \oint_{V_s} \vec{q} \cdot d\vec{s} = \overline{M}_k L_k q''$$ (2.4.4)

where $\overline{M}_k$ is the effective perimeter of the flow channel.

Substitution of Equation 2.4.2, 2.4.3 and 2.4.4 in Equation 2.4.1, yields

$$\frac{d}{dt}\int_V (\rho h)dV - A_k \rho_o h_o v_{so} + A_k \rho_i h_i v_{si} = - A_k \rho_o h_o v_o + A_k \rho_i h_i v_i$$

$$+ \overline{M}_k L_k q'' + \int_V \frac{\partial}{\partial t} P dV$$ (2.4.5)

Defining (ρh) as

$$(\rho h) = \int_V (\rho h)dV/(A_k L_k)$$ (2.4.6)

and recalling the definitions of the mass flux, Equation 2.2.5 and 2.2.6, one can rewrite Equation 2.4.6 as

$$\frac{d}{dt}(\rho h A_k L_k) = W_i h_i - W_o h_o + \overline{M}_k L_k q'' + \int_V \frac{\partial}{\partial t} P dV.$$ (2.4.7)

The last term in Equation 2.4.7 can be expanded, with the Leibnits' rule, as

$$\int_{V(t)} \frac{\partial}{\partial t} P dV = \frac{d}{dt}\int_{V(t)} P dV - A_k P_o v_{so} + A_k P_i v_{si}$$ (2.4.8)

or

$$\int_{V(t)} \frac{\partial}{\partial t} P dV = \frac{d}{dt}(A_k L_k \dot{P}) - A_k P_o v_{so} + A_k P_i v_{si}$$ (2.4.9)

where

$$\dot{P} = \int_V P dV / V_k .$$

The first term on the right hand side of Equation 2.4.9 can be rewritten as

$$\frac{d}{dt}(A_k L_k \dot{P}) = A_k L_k \frac{d}{dt}\dot{P} + A_k \dot{P}\frac{d}{dt}L_k \tag{2.4.10}$$

which with the expansion of the L_k as

$$L_k = s_o(t) - s_i(t)$$

becomes

$$\frac{d}{dt}(A_k L_k \dot{P}) = A_k L_k \frac{d}{dt}\dot{P} + A_k \dot{P}(v_{so} - v_{si}). \tag{2.4.11}$$

Inserting Equation 2.4.11 in Equation 2.4.9, one gets

$$\int_{V(t)} \frac{\partial}{\partial t} P dV = A_k L_k \frac{d}{dt}\dot{P} + A_k v_{so}(\dot{P} - P_o) + A_k v_{si}(P_i - \dot{P}). \tag{2.4.12}$$

Assuming $\dot{P} \cong (P_o + P_i)/2$, one gets for Equation 2.4.12, the expression

$$\int_{V(t)} \frac{\partial}{\partial t} P dV = A_k L_k \frac{d}{dt}\dot{P} + A_k(P_i - P_o)(v_{so} - v_{si}). \tag{2.4.13}$$

For operation transients, e.g., power reduction from 100% to 30% of the nominal power, within 30 seconds, the last term in Equation 2.4.13 is about three orders of magnitude smaller than the pressure variation term, thus it can be neglected.

Substitution of Equation 2.4.13, without the last term, in Equation 2.4.7 yields the energy conservation in the control volume V_k

$$\frac{d}{dt}(\rho h A_k L_k) = W_i h_i - W_o h_o + \overline{M}_k L_k q'' + A_k L_k \frac{d}{dt}\overline{P}. \tag{2.4.14}$$

3. STEAM GENERATOR MODELLING

The following paragraphs describe the modelling approximations adopted in the GVTRAN–PC program for simulating the most important phenomena that are observed in the U–tube steam generators. The primary and secondary side control volumes and the numerical approximations to the conservation equations will be described.

3.1   Control Volume Definition

The GVTRAN–PC program is written for the U–type steam generator schematically described in Figure 3.1.1 below.
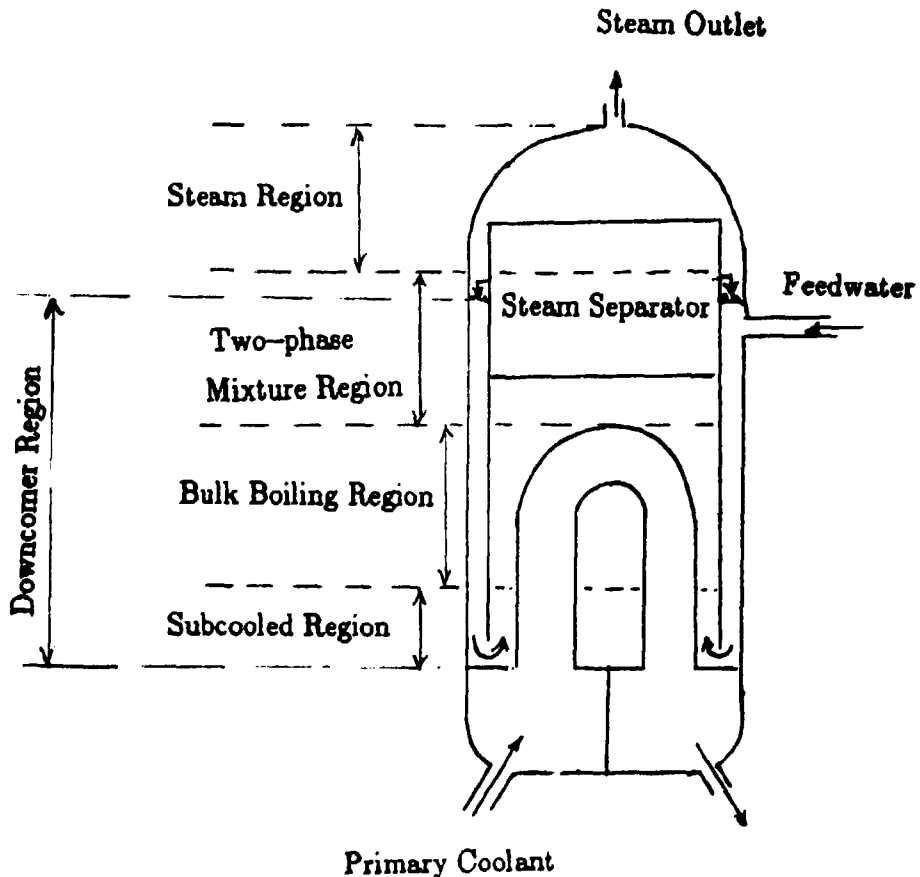
Steam Outlet

Figure 3.1.1 Illustration of the U–tube steam generator.

The control volumes defined in the steam generator are illustrated in Figure 3.1.2 below, where some significant parameters are shown schematically.
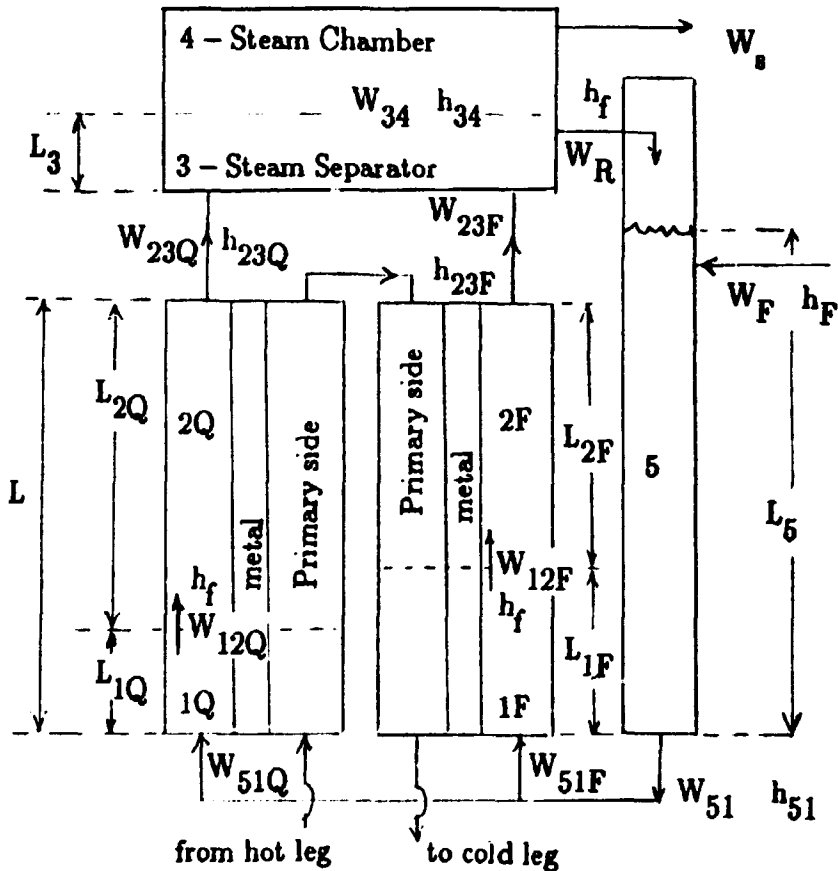

Figure 3.1.2 Control Volumes in the U–tube Steam Generator.

The flow areas in the secondary side, A_{1Q}, A_{2Q}, A_{1F} and A_{2F} are assumed as a constant and it is denoted by A_{tb}.

The total area for the regions 1Q and 1F will be denoted as

$$A_1 = A_{1Q} + A_{1F}$$

and similarly

$$A_2 = A_{2Q} + A_{2F} ,$$

noting, in addition, that $A_1 = A_2$ for the present steam generator modelling.

3.2 Mass Conservation Modelling

Equation 2.2.8 is rewritten, for clarity, as

$$W_i - W_o - \bar{\rho}_k A_k \frac{d}{dt} L_k - A_k L_k \frac{d}{dt} \bar{\rho}_k = 0 . \tag{3.2.1}$$

Subcooled Regions

The subcooled regions, 1Q and 1F, can be modelled with the simplifying assumptions by neglecting the time variation of the average density during the time span considered in the analysis. Equation 3.2.1 thus becomes

$$W_{12Q} = W_{51Q} - \rho_{1Q} A_{tb} \frac{d}{dt} L_{1Q} \tag{3.2.2-a}$$

$$W_{12F} = W_{51F} - \rho_{1F} A_{tb} \frac{d}{dt} L_{1F} \tag{3.2.2-b}$$

Bulk Boiling Region

In the bulk boiling region, disregarding the local boiling region, Equation 3.2.1 becomes

$$W_{23Q} = W_{12Q} - \rho_{2Q} A_{tb} \frac{d}{dt} L_{2Q} - A_{2Q} L_{2Q} \frac{d}{dt} \rho_{2Q} \tag{3.2.3}$$

and since $L = L_{1Q} + L_{2Q}$, that is,

$$\frac{d}{dt} L_{1Q} = -\frac{d}{dt} L_{2Q} ,$$

one gets

$$W_{23Q} = W_{12Q} + \rho_{2Q} A_{tb} \frac{d}{dt} L_{1Q} - A_{2Q} L_{2Q} \frac{d}{dt} \rho_{2Q} \tag{3.2.4-a}$$

and

$$W_{23F} = W_{12F} + \rho_{2F} A_{tb} \frac{d}{dt} L_{1F} - A_{2F} L_{2F} \frac{d}{dt} \rho_{2F} \tag{3.2.4-b}$$

where $\frac{d}{dt} \rho_{2Q}$ and $\frac{d}{dt} \rho_{2F}$ are described together with the void fraction model in Section 4.

The calculation results from the turbine trip transients in the Donald C. Cook Nuclear Station show the contribution of the compression term in the subcooled and saturated region.

In the subcooled region the terms of Equation 3.2.2–a and 3.2.2–b do not take into account the liquid expansion/contraction

$$- A_{tb} L_{1Q} \frac{d}{dt} \rho_{1Q} \quad \text{and} \quad - A_{tb} L_{1F} \frac{d}{dt} \rho_{1F}$$

since these terms contribute approximately with 20 kg/s during the 10 seconds of the transient simulation, whereas the last terms of Equation 3.2.2–a and 3.2.2–b contribute with 700 kg/s.

Contrariwise, the contribution of the expansion/contraction in the boiling region is relatively high, 200kg/s, when confronted with remaining terms which are of the order of 600kg/s and 300kg/s for W_{12} and the term representing the motion of the boiling point, respectively.

One can therefore conclude that the terms representing compression/expansion can not be neglected in the two–phase mixture region, consequently, neither in the vapor region.

Steam Separator

The steam separator mixture inflow, W_{23}, is the sum of W_{23Q} and W_{23F} mass flows, such that the mass conservation can be given as

$$W_{34} = W_{23} - W_R - \rho_3 A_3 \frac{d}{dt} L_3 - A_3 L_3 \frac{d}{dt} \rho_3 \qquad (3.2.5)$$

where $\frac{d}{dt}\rho_3$ term is developed together with the void fraction modelling.

The partial derivatives of L_{1Q}, L_{1F} and L_3 are obtained from the energy balance.

The recirculation flow is derived from the recirculation ratio R definition

$$R = \frac{W_{23}}{W_{23} - W_R} \qquad (3.2.6)$$

which can be obtained from the energy and momentum conservation.

Downcomer Region

In the *downcomer* region the mass conservation equation, Equation 3.2.1, will be

$$\frac{d}{dt}L_5 = \frac{W_F + W_R - W_{51}}{A_5\rho_5}$$ (3.2.7)

where $W_{51} = W_{51Q} + W_{51F}$.

3.3   Modelling the Energy Conservation

The energy conservation equation, Equation 2.4.14, is rewritten for clarity,

$$\frac{d}{dt}(\rho h A_k L_k) = W_i h_i - W_o h_o + S_k q'' + A_k L_k \frac{d}{dt}\dot{P},$$ (3.3.1)

where S_k is the heat transfer area for the control volume V_k.

Subcooled Region

In the subcooled region the terms corresponding to the time derivative of the enthalpy and density will be neglected, justified by a low dependence on pressure, and the pressure time derivative has found to be insignificant. Thus the energy conservation equation becomes

$$\frac{d}{dt}L_{1Q} = \frac{W_{51Q}h_{51} - W_{12Q}h_f + S_{1Q}q''}{A_{tb}\rho_{1Q}h_{1Q}}.$$ (3.3.2)

Substitution for W_{12Q} in Equation 3.3.2 with the expression given by Equação 3.2.2—a, one gets

$$A_{tb}\rho_{1Q}(h_{1Q} - h_f)\frac{d}{dt}L_{1Q} = W_{51Q}(h_{51} - h_f) + S_{1Q}q''.$$ (3.3.3)

If one assumes a linear enthalpy rise in the volume 1Q, h_{1Q} can be defined as an average of the input and output enthalpies,

$$h_{1Q} = (h_{51} + h_f)/2$$ (3.3.4)

and introducing h_{1Q} into Equation 3.3.3, one gets

$$\frac{d}{dt}L_{1Q} = \frac{2W_{51Q}}{t\,b\,\prime_{1Q}} + \frac{S_{1Q}q^{\kappa}}{A_{tb}\prime_{1Q}(h_{1Q} - h_f)} \tag{3.3.5}$$

Similar expression is obtained for the cold leg region.

Bulk Boiling Region

In the bulk boiling region both the enthalpy variation term and the compression term are considered, such that the energy conservation equation can be rewritten as

$$\frac{d}{dt}(M_{2Q}h_{2Q}) = W_{12Q}h_f - W_{23Q}h_{23Q} + M_{2Q}L_{2Q}q''_{2Q} + \frac{A_{tb}L_{2Q}}{J}\frac{d}{dt}P_{2Q} \tag{3.3.6}$$

where J is the conversion factor(10^{-5}bar/Pa).

Under linear enthalpy rise assumption the enthalpy h_{2Q} can be written as

$$h_{2Q} = (h_{23Q} + h_f)/2 \tag{3.3.7}$$

which allows the expression for h_{23Q} to be written as

$$h_{23Q} = 2h_{2Q} - h_f . \tag{3.3.8}$$

With the substitution for h_{23Q}, Equation 3.3.8, into Equation 3.3.6, one gets

$$M_{2Q}\frac{d}{dt}h_{2Q} = -h_{2Q}\frac{d}{dt}M_{2Q} + W_{12Q}h_f - W_{23Q}(2h_{2Q} - h_f)$$
$$+ M_{2Q}L_{2Q}q''_{2Q} + \frac{A_{tb}L_{2Q}}{J}\frac{d}{dt}P_{2Q} \tag{3.3.9}$$

which itself, after the substitution of the first term on the right hand side with the mass conservation equation, Equation 2.2.7, and also admitting P_{2Q} as the steam pressure P_s, becomes

$$\frac{d}{dt}h_{2Q} = [-(h_{2Q} - h_f)(W_{23Q} + W_{12Q}) + M_{2Q}L_{2Q}q''_{2Q}$$
$$+ \frac{A_{tb}L_{2Q}}{J}\frac{d}{dt}P_s]/M_{2Q} \tag{3.3.10}$$

Similar expression is obtained for the cold leg region.

Steam Separator

The steam separator, represented by volume 3, presents as an input enthalpy, the weighted average of the exit enthalpies from the region 2Q and 2F,

$$h_{23} = \frac{W_{23Q} h_{23Q} + W_{23F} h_{23F}}{W_{23Q} + W_{23F}} \tag{3.3.11}$$

with steam quality given by

$$X_{23} = (h_{23} - h_f)/h_{fg} \tag{3.3.12}$$

The energy conservation equation, Equation 2.4.14, for region 3, becomes

$$\frac{d}{dt}(\rho_3 h_3 A_3 L_3) = W_{23} h_{23} - W_R h_f - W_{34} h_g + \frac{A_3 L_3}{J}\frac{d}{dt}P_s \tag{3.3.13}$$

The time derivative of h_3 can be neglected in view of the time derivative of L_3, such that, with the substitution of W_{34} from Equation 3.2.5, Equation 3.3.13 becomes

$$A_3 \rho_3 (h_g - h_{23})\frac{d}{dt}L_3 = W_{23}(h_g - h_{23}) - W_R(h_g - h_f)$$

$$- \frac{A_3 L_3}{J}\frac{d}{dt}P_s , \tag{3.3.14}$$

where the enthalpy h_3 was taken as the input enthalpy h_{23}, given the low contribution of the compression term.

In Section 6 it will be shown that h_{23} can be given as

$$h_{23} = h_f + \chi_s h_{fg}/R \tag{3.3.15}$$

which inserted in Equation 3.3.14 results in

$$\frac{d}{dt}L_3 = \frac{W_{23}}{A_3 \rho_3} - \frac{\left[\frac{R^s}{R-1}\right]}{A_3 \rho_3 h_{fg}}\left[W_R h_{fg} + \frac{A_3 L_3}{J}\frac{d}{dt}P_s\right] \tag{3.3.16}$$

where $R^* = R/\chi_s$, and χ_s is the steam quality at the steam generator outlet.

Steam Chamber

The conservation equations for the region 4 are derived by balancing the mass and energy in volume 3 and 4 simultaneously, once the variable L_3 is a moving boundary.

Denoting the total liquid volume as V_L and the total steam volume as V_G, one can write for the resulting sum of the volume 3 and 4,

$$V_T = V_L + V_G \tag{3.3.17}$$

and

$$V_L = (1 - \alpha_3)A_3 L_3 , \tag{3.3.18}$$

such that

$$\frac{d}{dt}V_L = -\frac{d}{dt}V_G . \tag{3.3.19}$$

The mass conservation equation, Equation 2.2.7, developed for volume 3 and 4 results in

$$\frac{d}{dt}[V_L \rho_f + V_G \rho_g] = W_{23} - W_R - W_s . \tag{3.3.20}$$

Since the saturation state is assumed, that is,

$$\rho = \rho(P) \tag{3.3.21-a}$$

and

$$\frac{d}{dt}\rho = (\frac{d}{dP}\rho)(\frac{d}{dt}P) . \tag{3.3.21-b}$$

by using Equation 3.3.19 and 3.3.21-b, Equation 3.3.20 becomes

$$\frac{d}{dt}V_L = \frac{1}{\rho_f \rho_g}[W_{23} - W_R - W_s - (V_L \frac{d}{dP}\rho_f + V_G \frac{d}{dP}\rho_g)\frac{d}{dt}P] .$$

$$\tag{3.3.22}$$

Equation 2.4.14, the energy conservation equation, defined in volume 3 and 4, results in

$$\frac{d}{dt}(V_L \rho_f h_f + V_G \rho_g h_g) = W_{23} h_{23} - W_R h_f - (1 - \chi_s) W_s h_f$$

$$-\chi_s W_s h_g + \frac{V_T}{J} \frac{d}{dt} P_s .$$ (3.3.23)

Considering in the saturation state, in addition to Equation 3.3.21-a and 3.3.21-b, one gets

$$h = h(P)$$ (3.3.24-a)

and

$$\frac{d}{dt} h = (\frac{d}{dP} h)(\frac{d}{dt} P) .$$ (3.3.24-b)

Rearranging Equation 3.3.23 making use of Equation 3.3.21, 3.3.24, and 3.3.22, one gets

$$\frac{d}{dt} P_s = \{ W_{23} h_{23} - W_R^* h_f - W_s^* h_g - \frac{(\rho_f h_f - \rho_g h_g)}{(\rho_f - \rho_g)} (W_{23} - W_R - W_s) \}/$$

$$\{ V_L (h_f \frac{d}{dP} \rho_f + \rho_f \frac{d}{dP} h_f) + V_G (h_g \frac{d}{dP} \rho_g + \rho_g \frac{d}{dP} h_g)$$

$$- \frac{(\rho_f h_f - \rho_g h_g)}{(\rho_f - \rho_g)} (V_L \frac{d}{dP} \rho_f + V_G \frac{d}{dP} \rho_g) - \frac{V_T}{J} \}$$ (3.3.25)

where $W_R^* = W_R + (1 - \chi_s) W_s$ and $W_s^* = \chi_s W_s$;
or rearranging the terms

$$\frac{d}{dt} P_s = \{ [h_{23} - \frac{(\rho_f h_f - \rho_g h_g)}{(\rho_f - \rho_g)}] W_{23} - \frac{\rho_g}{(\rho_f - \rho_g)} h_{fg} W_R^* - \frac{\rho_f}{(\rho_f - \rho_g)} h_{fg} W_s^* \}/$$

$$\{ V_L \rho_f \frac{d}{dP} h_f + V_G \rho_g \frac{d}{dP} h_g + V_L (\frac{d}{dP} \rho_f) \frac{\rho_g}{(\rho_f - \rho_g)} h_{fg} +$$

$$V_G (\frac{d}{dP} \rho_g) \frac{\rho_f}{(\rho_f - \rho_g)} h_{fg} - \frac{V_T}{J} \}$$ (3.3.26)

One can notice that χ_s, the steam quality at the steam generator outlet, whereas considered in the pressure calculation, in the normal operation condition is negligible.

Alternatively the pressure was calculated with the volume conservation, as described below, and an alternative GVTRAN-PC version was also developed.

In this model the steam separator region, region 3, is fixed and equations considered are for the liquid and steam volume conservation, V_L and V_G,

$$\frac{d}{dt}(V_L + V_G) = 0 = v_L\frac{d}{dt}M_L + M_L\frac{d}{dt}v_L + v_G\frac{d}{dt}M_G + M_G\frac{d}{dt}v_G \; ;$$

and for the liquid and vapor energy conservation

$$\frac{d}{dt}(M_L h_L) = (W_L h_L)_i - (W_L h_L)_o + v_L\frac{d}{dt}P$$

and

$$\frac{d}{dt}(M_G h_G) = (W_G h_G)_i - (W_G h_G)_o + V_G\frac{d}{dt}P \; .$$

The specific volume variations can be expressed as

$$\frac{d}{dt}v_L = (\frac{d}{dP}v_L)_{h_L}\frac{d}{dt}P + (\frac{d}{dh_L}v_L)_P\frac{d}{dt}h_L$$

and

$$\frac{d}{dt}v_G = (\frac{d}{dP}v_G)_{h_G}\frac{d}{dt}P$$

if one assumes saturated steam in the steam chamber.

With the substitution of the expressions of $\frac{d}{dt}v_L$ and $\frac{d}{dt}v_G$ into the volume conservation equation, and with the substitution for $\frac{d}{dt}h_L$ and $\frac{d}{dt}h_G$ obtained from the energy equation, the final expression becomes

$$\frac{d}{dt}P = - \{v_L\frac{d}{dt}M_L + v_G\frac{d}{dt}M_G + (\frac{d}{dh_L}v_L)_P[(W_L h_L)_i - (W_L h_L)_o -$$

$$h_L\frac{d}{dt}M_L\}/\{M_L(\frac{d}{dP}v_L)_{h_L} + M_G(\frac{d}{dP}v_G)_{h_G} + V_L(\frac{d}{dh_L}v_L)_P\} \; .$$

Schematically the steam chamber is illustrated in Figure 3.3.1.

If one assumes the enthalpy h_L as the saturated liquid enthalpy, h_f, the last term in the numerator is zeroed, because

$$(W_L h_L)_i - (W_L h_L)_o = h_f(W_{L_i} - W_{L_o}) = h_f\frac{d}{dt}M_L \; .$$

Since $\frac{d}{dt}M_L = W_{L_i} - W_{L_o}$

and $\quad \frac{d}{dt}M_G = W_{G_i} - W_{G_o}$, the equation for the pressure becomes

$$\frac{d}{dt}P = -\{v_L[(1 - x_{23})W_{34} + W_F - W_{51}] + v_G[x_{23}W_{34} - W_{sGV}]\}/$$

$$\{V_L\rho_f(\frac{d}{dP}v_L)_{h_L} + V_G\rho_g(\frac{d}{dP}v_G)_{h_G} + V_L(\frac{d}{dh_L}v_L)P\}.$$
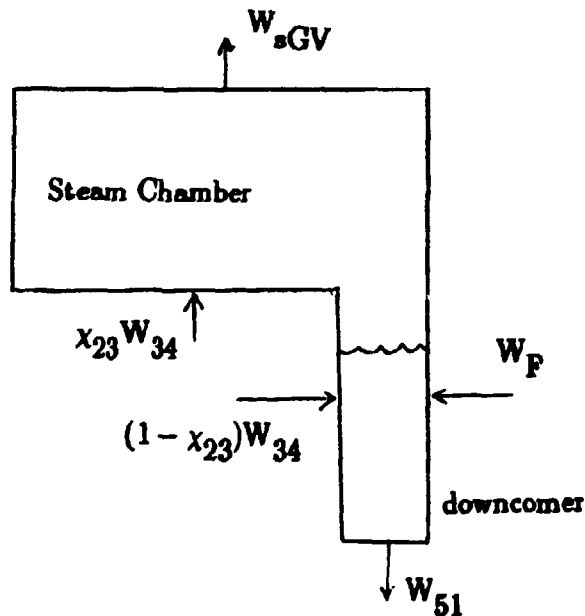

Figure 3.3.1 Steam Chamber Model for the Steam Generator.

The expression for W_{34} , in the alternative model, differs from Equation 3.2.5, and it is given as

$$W_{34} = W_{23} - V_3\frac{d}{dt}\rho_3.$$

Tests were performed to assess the effect of the contraction/expansion term in the separator, and it was noticed that its effect on the water level in the

downcomer is significant: difference up to 20% in the water level variation during the Donald C. Cook turbine trip transient.

Downcomer Region

The energy conservation equation, Equação 2.4.14, applied to region 5, yields

$$\frac{d}{dt}(\rho_f h_5 A_5 L_5) = W_F h_F + W_R h_f - W_{51} h_{51} \tag{3.3.27}$$

by observing that the fluid density is considered constant in the subcooled region, and moreover, that it is calculated subject to the steam dome pressure, P_s, in a saturation state.

Recalling the time derivative expression for L_5, Equation 3.2.7, Equation 3.3.27 can be rewritten as

$$\frac{d}{dt} h_5 = \frac{1}{\rho_f A_5 L_5} \{ W_F h_F + W_R h_f - W_{51} h_{51} - h_5(W_F - W_R - W_{51}) \} \tag{3.3.28}$$

or $\frac{d}{dt} h_5 = \frac{1}{\rho_f A_5 L_5} \{ W_F(h_F - h_5) + W_R(h_f - h_5) - W_{51}(h_{51} - h_5) \}$.

$$\tag{3.3.29}$$

This downcomer model has shown to be completely inadequate when compared with the known experimental results.

Section 8 presents the improved downcomer model implemented in the final GVTRAN-PC version.

Primary Side Regions

Density variations are neglected in the primary side region, because the model developed is applicable only to the conditions close to the operating conditions.

The equations in the control volumes are all identical in the primary side, therefore an arbitrary control volume V_k will be balanced below.

From the mass conservation equation, Equation 2.2.7, one gets

$$\frac{d}{dt}(\rho_k A_k L_k) = W_i - W_o \tag{3.3.30}$$

and from the energy conservation equation, Equation 2.4.14,

$$\frac{d}{dt}(\rho_k h_k A_k L_k) = W_i h_i - W_o h_o - \dot{Q} \tag{3.3.31}$$

which can be rewritten as,

$$\frac{d}{dt}h_k = \frac{1}{M_k}[W_i h_i - W_o h_o - \dot{Q} - h_k \frac{d}{dt}(\rho_k A_k L_k)] . \tag{3.3.32}$$

Substitution of the last term on the right hand side of Equation 3.3.32 with the expression 3.3.30, results in

$$\frac{d}{dt}h_k = \frac{1}{M_k}[W_i(h_i - h_k) - W_o(h_o - h_k) - \dot{Q}] \tag{3.3.33}$$

where $\dot{Q}$ is the heat flux into the metallic region.

Primary Side Temperature

The primary side regions are defined in Figure 3.3.2 below, with the following approximations:

— constant pressure,
— constant density, thus constant flow rate, and
— constant specific heat.

The equations implemented are derived from the following differential equations:

$$\frac{d}{dt}T_{4Asat} = \frac{1}{\rho_f A_{1p} L_1 c_p}[Wc_p(T_{pqA} - T_{4Asat}) - Q_{tot1A}]$$

$$\frac{d}{dt}T_{4A} = \frac{1}{\rho_f A_{2p} L_2 c_p}[Wc_p(T_{4Asat} - T_{4A}) - Q_{tot2A}]$$

$$\frac{d}{dt}T_{5Asat} = \frac{1}{\rho_f A_{2p} L_2 c_p} [\, Wc_p(T_{4A} - T_{5A}) - Q_{tot2B}]$$

$$\frac{d}{dt}T_{5A} = \frac{1}{\rho_f A_{1p} L_1 c_p} [\, Wc_p(T_{5Asat} - T_{5A}) - Q_{tot1B}]\,.$$
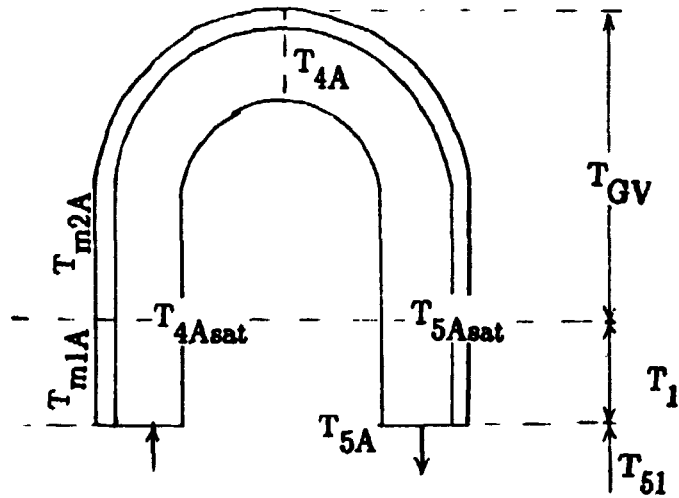
Figure 3.3.2 Primary Side Region in the Steam Generator.

Metallic Tube Region

The heat conduction equation, without the radiation heat transfer, is given as

$$\frac{\partial}{\partial t}(\rho c_p T) + \nabla \cdot q'' = S(\vec{r}, t)\,. \tag{3.3.34}$$

Integrating Equation 3.3.34 in the control volume V_k, and neglecting the axial conduction, one gets

$$\frac{d}{dt}(M_k c_p T) = \dot{Q}_i - \dot{Q}_o \tag{3.3.35}$$

where

$\dot{Q}_i$ is the heat flux into V_k, and

$\dot{Q}_o$ is the heat flux from V_k.

The heat flux is computed based on the average temperature in the metallic tube defined at its midpoint, as shown in the Figure 3.3.3 below.
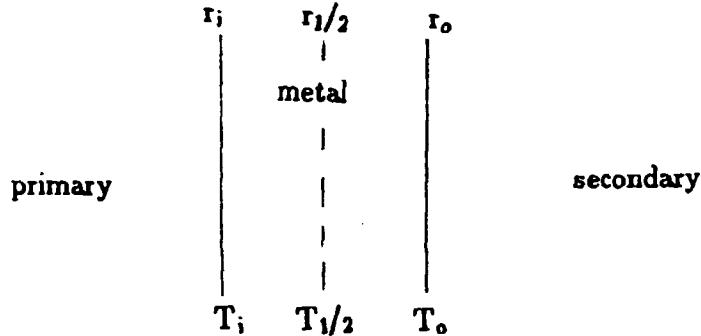

Figure 3.3. 3 Definition of Temperature in the Metallic Tube.

The steady state temperature distribution in a cylindrical geometry is given as

$$T(\vec{r}) = T_{ref} + \frac{A}{k_m}\ln(1 + \frac{\Delta r}{r_{ref}})$$

(3.3.36)

where

T_{ref} = temperature at r_{ref}, $r_i \leq r_{ref} \leq r_o$,

A = $-r_i q''_{prim}$ = $-r_o q''_{sec}$

Δr = $|\vec{r} - \vec{r_i}|$,

that is, it is a solution of the Laplace's equation with constant k_m,

$$\frac{1}{r}\frac{d}{dr}r\ k_m \frac{d}{dr}T(r) = 0 .$$

The resistance between the primary and secondary side of the steam generator is divided in two parts, with the common boundary at the midpoint of the metallic tube as shown in the figure above.

On the left hand side, i.e., the primary side, the resistances are described by the approximate equations, as

$$\Delta T_{film\ in\ primary} = q''_{prim} (\ 1/h_{prim} + R_{fouling\ prim})$$

where

h_{prim} = convective heat transfer coefficient on the primary side,

$R_{fouling \atop prim}$ = fouling resistance.

and

$$\Delta T_{left \atop metallic \atop tube} = q''_{prim} \frac{r_i}{k_m} \ln(\frac{r_{1/2}}{r_i}) \approx \frac{\Delta R}{2k_m}$$

where

$$r_{1/2} = \frac{1}{2}(r_i + r_o)$$
$$\Delta R = (r_o - r_i)$$

presenting therefore, in the primary side region, the effective heat conduction coefficient given by

$$\frac{1}{U_{prim}} = \frac{1}{h_{prim}} + R_{fouling \atop prim} + \frac{r_i}{k_m} \ln(\frac{r_{1/2}}{r_i}) . \qquad (3.3.37)$$

Analogously, in the secondary side regions, i.e., in the right hand side region the effective heat conduction coefficient is given by

$$\frac{1}{U_{sec}} = \frac{1}{h_{sec}} + R_{fouling \atop sec} + \frac{r_o}{k_m} \ln(\frac{r_o}{r_{1/2}}) , \qquad (3.3.38)$$

making use of the expression

$$T_o = T_{1/2} - q''_{sec} \frac{r_o}{k_m} \ln(\frac{r_o}{r_{1/2}})$$

where $R_{fouling \atop sec} = 8.8 \times 10^{-6} \, °C/W/m^2$.

The heat fluxes, $\dot{Q}_i$ and $\dot{Q}_o$, are, therefore, given by

$$\dot{Q}_i = M_{prim} L_k U_{prim} (T_{prim} - T_{metal}) \qquad (3.3.39)$$

and

$$\dot{Q}_o = M_{sec} L_k U_{sec} (T_{metal} - T_{sec}) \qquad (3.3.40)$$

where M_{prim} and M_{sec} are the wet perimeter in the primary and secondary side regions.

Why One Control Volume?

The energy conservation in the tube region was implemented by considering only one control volume. The question regarding the extent of its validity is discussed below based on the analysis of the control volume time constant.

From Equation 3.3.35 one gets

$$Mc_p\frac{d}{dt}T_m = U_{prim} \text{ Per } L \ (T_{prim} - T_m) - U_{sec} \text{ Per } L \ (T_m - T_{sec}),$$

or $\frac{d}{dt}T_m \approx -(U_{prim} + U_{sec})\text{Per } L \ T_m/(M \ c_p) = - T_m/\tau$

where

$$\tau = \frac{M \ c_p}{(U_{prim} + U_{sec}) \text{ Per } L} \ .$$

The value of the time constant τ is estimated with the substitution for the D.C.Cook steam generator parameters,

$$M \approx 23000 kg$$
$$c_p \approx 500J/kg/^oC$$
$$\text{Per} \approx 230\text{m}$$
$$L \approx 10\text{m}$$
$$(U_{prim} + U_{sec})) \approx 24000J/s/m^2/^\circ C,$$

and it results in $\tau \approx 0.2$ seconds.

Therefore the time constant of one control volume is sufficiently small permitting the implementation of one control volume scheme.

4 AVERAGE VOID FRACTION, $\bar{a}$, AND $\frac{d}{dz}\rho$

The void fraction in the two-phase flow regions can be computed with one of the following approximations, e.g., homogeneous model, slip-flow model or drift-flux model. A particular choice will be based on the required sensibility, computational availability, and regimen of flow predominant in the control volume considered.

Homogeneous Model

In the homogeneous model the phase velocities are assumed uniform,

$$\vec{v}_g = \vec{v}_f = \vec{v} \ ;$$

and following parameters of interest are defined:

$$\chi(z) = \frac{W_g(z)}{W_g(z) + W_f(z)} = \frac{h(z) - h_f}{h_{fg}} \tag{4.1}$$

$$\alpha(z) = \frac{(\rho_f/\rho_g)\,\chi(z)}{1 + \chi(z)(\rho_f/\rho_g - 1)} \tag{4.2}$$

$$\rho = \alpha\rho_g + (1 - \alpha)\rho_f \ . \tag{4.3}$$

Slip-flow Model

In the slip-flow approximation the phase velocities are distinct such that this model is recommended for use in the high void fraction flow regimen. Few definitions will be explained before the presentation of the void fraction models.

The slip factor S is defined as

$$S = v_g/v_f \tag{4.4}$$

that is

$$S = \frac{\chi(1 - \alpha)}{(1 - \chi)\alpha}\frac{\rho_f}{\rho_g} \tag{4.5}$$

In terms of the void fraction α, W_g and W_f are given as

$$W_g = \alpha \rho_g v_g A \qquad (4.6)$$

$$W_f = (1 - \alpha) \rho_f v_f A \qquad (4.7)$$

Defining γ as

$$\gamma = \frac{1}{S} \frac{\rho_f}{\rho_g} \qquad (4.8)$$

one gets the expression for the void fraction

$$\alpha(z) = \frac{\gamma \chi(z)}{1 + \chi(z) (\gamma - 1)} . \qquad (4.9)$$

The values of γ are tabulated as a function of pressure in Reference 1, and they are correlated to the specific volumes, v_g and v_f, through the following expression, in the range 250–1250 psia(17–86 bar),

$$\gamma = 1.26 (v_g/v_f)^{0.75} \qquad (4.10)$$

or approximately as

$$\gamma = 630/P(bar) \qquad (4.11)$$

for pressures around 40 bar.

Drift–Flux Model

The drift–flux model is appropriate for the flow regimens characterised as annular or plug flow.

In the drift–flux model the volumetric flow are defined as

$$j_f = Q_f/A = (1 - \alpha)v_f \qquad (4.12\text{-a})$$

$$j_g = Q_g/A = \alpha v_g \qquad (4.12\text{-a})$$

where Q_f and Q_g are the volume flow per unit time for fluid and gas, respectively.

The average volumetric velocity is defined as

$$j = (Q_f + Q_g)/A \qquad (4.13)$$

and the drift-flux and the drift velocity as

$$j_{21} = \alpha \, (v_g - j) \qquad (4.14)$$

and

$$v_{DF} = v_g - j = (1 - \alpha) \, (v_g - v_f) \; , \qquad (4.15)$$

respectively, which combined yield the expression

$$j_{21} = \alpha \, v_{DF} = (1 - \alpha) \, j_g - \alpha \, j_f \cdot \qquad (4.16)$$

That is, j_{21} is the void volumetric flux relative to a plane moving with the velocity j, and j_{12} equals $-j_{21}$, where j_{21} is the fluid volumetric flux incident on the the same plane. v_{DF} is the drift velocity of the void relative to the average volume velocity j.

From the definition of j, Equation 4.13, one gets

$$j = j_g + j_f \qquad (4.17)$$

which combined with Equation 4.16 results in

$$\alpha = \frac{j_g}{j} \, (1 - \frac{j_{21}}{j_g}) \qquad (4.18)$$

or rearranging Equation 4.16, with the help of Equation 4.17, the result is

$$\alpha(z) = \frac{j_g(z)}{j(z) + v_{DF}} \cdot \qquad (4.19)$$

In the practice, however, the measured and analyzed quantities are the average quantities in the flow area. That is,

$$v_g = \frac{\int_A \alpha(\vec{r}) \, v_g(\vec{r}) \; dA}{\int_A \alpha(\vec{r}) \, dA} \qquad (4.20)$$

and

$$\bar{v}_{DF} = \frac{\int_A \alpha(\vec{r}) \, v_{DF}(\vec{r}) \, dA}{\int_A \alpha(\vec{r}) \, dA} \qquad (4.21)$$

or, with the substitution of v_{DF} from Equation 4.15,

$$\bar{v}_{DF} = \frac{\int_A \alpha(\vec{r}) \, v_g(\vec{r}) \, dA}{\int_A \alpha(\vec{r}) dA} - \frac{\int_A \alpha(\vec{r}) \, j(\vec{r}) \, dA}{\int_A \alpha(\vec{r}) dA} . \qquad (4.22)$$

By defining a factor of void concentration along the radial position as

$$C_o = \left[\frac{\int_A \alpha(\vec{r}) \, j(\vec{r}) \, dA}{\int_A \alpha(\vec{r}) dA} \right] / \alpha \qquad (4.23)$$

where $\qquad \alpha = \int_A \alpha(\vec{r}) dA / A$,

one gets from Equation 4.22

$$\bar{v}_{DF} = v_g - C_o j . \qquad (4.24)$$

Comparing Equation 4.15 and 4.24, one conclude

$$v_{DF} = \bar{v}_{DF} + (C_o - 1) j ; \qquad (4.25)$$

which inserted in 4.19, yields an usable expression for the void fraction

$$\alpha(z) = \frac{j_g(z)}{C_o j(z) + \bar{v}_{DF}} . \qquad (4.26)$$

The correlations are obtained experimentally, vis. TRAC–PD2 correlations :

$$\bar{v}_{DF} = \begin{cases} 1.41 \, [g\sigma \, \frac{(\rho_f - \rho_g)}{\rho_f^2}]^{1/4} & \text{for } 0.01 < \alpha < 0.1 \\[2ex] 0.35 \, [g(\rho_f - \rho_g)\frac{D_e}{\rho_f}]^{1/2} & \text{for } 0.2 < \alpha < 0.65 \\[2ex] 0.0 & \text{for } \alpha < 0.01 \text{ and } \alpha = 1.0 \end{cases}$$

and the correlation for C_o utilised in THOR code:

$$C_o = \begin{cases} 1 + 0.19(1 - P/P_{crit})^{2.4} & \text{for } 0.2 < \alpha < 0.65 \\ \\ 1 & \text{for } \alpha < 0.01 \text{ and } \alpha > 0.85 \end{cases}$$

In both correlations the values in the intermediate range are linearly interpolated.

Therefore, the parameters required for evaluating the void fraction $\alpha(s)$, using Equation 4.26, are only the volumetric fluxes, which are obtained from the expressions

$$j_g(s) = \frac{\dot{Q}_2}{\rho_g \, h_{fg} \, A_2} \frac{(s - L_1)}{L_2} \quad , \tag{4.27}$$

$$j_f(s) = \frac{W_{51}}{\rho_f \, A_2} - \frac{\rho_g}{\rho_f} j_g \quad , \tag{4.28}$$

and

$$j(s) = \frac{W_{51}}{\rho_f \, A_2} + (1 - \frac{\rho_g}{\rho_f}) \, j_g(s) \tag{4.29}$$

where

$$L_1 = (L_{1Q} + L_{1F})/2 ,$$
$$L_2 = (L_{2Q} + L_{2F})/2 ,$$

$$\dot{Q}_2 = (q''_{2Q} + q''_{2F}) \cdot (\text{heat transfer area in regions 2Q and 2F}) , \text{ and}$$
$$A_2 = A_{2Q} + A_{2F} .$$

Once the void fraction, $\alpha(s)$, is calculated in the boiling region it is possible to estimate the average void fraction, $\bar{\alpha}$, by assuming an enthalpy rise profile.

In the approximation a linear enthalpy gain along the bulk boiling flow channel is assumed. It is recognized as a realistic assumption and no significant discrepancy should be expected in the values of $\bar{\alpha}$.

Therefore, one assumes

$$\chi(s) = \frac{s - L_1}{L_2} \, \chi_{23} \qquad (4.30)$$

and $\bar{\alpha}$ is defined as

$$\bar{\alpha} = \frac{1}{L_2} \int_{L_1}^{L} \alpha(s) \, ds \ . \qquad (4.31)$$

4.1 $\bar{\alpha}$ – Homogeneous Model

The average void fraction in homogeneous model is immediately derived from Equation 4.2.4 below, with the substitution of γ given by

$$\gamma = \frac{\rho_f}{\rho_g}$$

i.e., assuming unity for S, that is, single velocity.

4.2 $\bar{\alpha}$ – Slip–Flow Model

Substitution of Equation 4.9 into 4.31 results in

$$\bar{\alpha} = \frac{1}{L_2} \int_{L_1}^{L} \frac{\gamma \chi(s)}{1 + \chi(s)\,(\gamma - 1)} \, ds \qquad (4.2.1)$$

which with a change of variable by using Equation 4.30

$$d\chi(s) = \frac{\chi_{23}}{L_2} \, ds \ .$$

results in

$$\bar{\alpha} = \frac{1}{\chi_{23}} \int_{0}^{\chi_{23}} \frac{\gamma \chi(s)}{1 + \chi(s)\,(\gamma - 1)} \, d\chi \ . \qquad (4.2.2)$$

With a new change of variable

$$y = 1 + (\gamma - 1)\chi$$

Equation 4.2.2 becomes

$$\bar{\alpha} = \frac{\gamma}{\chi_{23}(\gamma-1)^2} \int_{1}^{1+(\gamma-1)\chi_{23}} (1 - 1/y)\, dy \qquad (4.2.3)$$

which by integration results in the expression for average void fraction in the slip–flow model

$$\bar{\alpha} = \frac{\gamma}{\gamma-1}\left[1 - \frac{\ln\{1 + (\gamma-1)\chi_{23}\}}{(\gamma-1)\chi_{23}}\right]. \qquad (4.2.4)$$

4.3 $\bar{\alpha}$ – Drift–Flux Model

In the drift–flux model the expression for the average void in the bulk boiling region becomes

$$\bar{\alpha} = \frac{1}{L_2}\int_{L_1}^{L} \frac{j(s)}{C_o\, j(s) + \bar{v}_{DF}}\, ds . \qquad (4.3.1)$$

Substituting Equation 4.29 in 4.3.1 one gets

$$\bar{\alpha} = \frac{1}{L_2}\int_{L_1}^{L} \frac{j_g(s)}{\dfrac{C_o W_{51}}{\rho_f A_2} + C_o(1 - \dfrac{\rho_g}{\rho_f})j_g(s) + \bar{v}_{DF}}\, ds . \qquad (4.3.2)$$

With change of variable based on Equation 4.27

$$dj_g(s) = \frac{\dot{Q}_2}{\rho_g\, h_{fg}\, A_2\, L_2}\, ds$$

Equation 4.3.2 is given as the expression

$$\bar{\alpha} = \frac{\rho_g h_{fg} A_2}{\dot{Q}} \int_0^{j_g(L)} \frac{j_g(z)}{\frac{C_o W_{61}}{\rho_f A_2} + C_o(1 - \frac{\rho_g}{\rho_f})j_g(z) + \bar{v}_{DF}} \, dj_g(z) \ .$$

(4.3.3)

After a change of variable

$$y = \frac{C_o W_{61}}{\rho_f A_2} + C_o(1 - \rho_g/\rho_f)j_g(z) + \bar{v}_{DF}$$

it is rewritten as

$$\bar{\alpha} = \frac{\rho_g h_{fg} A_2}{\dot{Q}_2 C_o^2 (1 - \rho_g/\rho_f)^2} \int_{y_1}^{y_2} [1 - \frac{(\frac{C_o W_{61}}{\rho_f A_2} + \bar{v}_{DF})}{y}] \, dy$$

(4.3.3)

with

$$y_1 = \frac{C_o W_{61}}{\rho_f A_2} + \bar{v}_{DF} \ ,$$

$$y_2 = y_1 + C_o(1 - \rho_g/\rho_f) \, j_g(L) \ ,$$

$$j(L) = \dot{Q}_2/(\rho_g h_{fg} A_2) \ ,$$

which by integration becomes:

$$\bar{\alpha} = \frac{1}{C_o(1 - \rho_g/\rho_f)} - \frac{(\frac{C_o W_{61}}{\rho_f A_2} + \bar{v}_{DF})}{j_g(L)[C_o(1 - \rho_g/\rho_f)]^2} \ln\left[1 + \right.$$

$$\left. \frac{C_o(1 - \rho_g/\rho_f)}{\frac{C_o W_{61}}{\rho_f A_2} + \bar{v}_{DF}} j_g(L) \right] \ .$$

(4.3.4)

But assuming $j_g \gg j_f$, and performing an integration in Equation 4.3.1 with $j(s) = j_g(s)$, the final expression is

$$\bar{a} = \frac{1}{C_o} - \frac{\bar{v}_{DF}}{j_g(L) C_o^2} \ln[1 + \frac{C_o j_g(L)}{\bar{v}_{DF}}]$$

(4.3.5)

4.4 Estimative of $\frac{d}{dt}\rho_2$ and $\frac{d}{dt}\rho_3$

The expressions for $\frac{d}{dt}\rho_2$ and $\frac{d}{dt}\rho_3$ below are based on the slip-flow approximation.

Since one assumes a constant void fraction equal to α_{23} in the steam separator one gets

$$\rho_3 = \alpha_3 \rho_g + (1 - \alpha_3) \rho_f$$

and, thus, its time derivative as

$$\frac{d}{dt}\rho_3 = \alpha_3 \frac{d}{dt}\rho_g + (1 - \alpha_3) \frac{d}{dt}\rho_f + (\rho_g - \rho_f) \frac{d}{dt}\alpha_3 .$$

Considering

$$\alpha_3 = \frac{\gamma \; x_{23}}{1 + x_{23}(\gamma - 1)} \qquad \text{and} \qquad \gamma = \frac{830}{P(bar)} ,$$

one gets $\quad \frac{1}{\gamma}\frac{d}{dP}\gamma = -\frac{1}{P}$,

hence with the final expression as

$$\frac{d}{dt}\rho_3 = [\alpha_3 \frac{d}{dP}\rho_g + (1 - \alpha_3) \frac{d}{dP}\rho_f + (\rho_g - \rho_f)\frac{d}{dP}\alpha_3] \frac{d}{dt}P$$

(4.4.1)

where

$$\frac{d}{dP}\alpha_3 = - \alpha_3 (1 - \alpha_3)/P$$

40

and

$$\frac{d}{dP}\rho_k = -\rho^2 \frac{d}{dP}v_k \qquad\qquad , k = f,g .$$

A similar expression can be deduced for $\frac{d}{dt}\rho_2$, as

$$\frac{d}{dt}\rho_2 = [\alpha_2 \frac{d}{dP}\rho_g + (1 - \alpha_2) \frac{d}{dP}\rho_f + (\rho_g - \rho_f)\frac{d}{dP}\alpha_2] \frac{d}{dt}P .$$

(4.4.2)

Recalling that α_2 is the average void fraction in region 2,

$$\alpha_2 = \frac{\gamma}{\gamma-1} \left[1 - \frac{\ln\{1 + (\gamma-1)\ \chi_{23}\}}{(\gamma - 1)\ \chi_{23}} \right] \quad ,$$

one gets

$$\frac{d}{dP}\alpha_2 = \frac{\gamma_2}{(\gamma - 1)P} - \frac{\gamma^2}{P(\gamma - 1)^2 \chi_{23}} \left[\frac{\ln\{1 + (\gamma-1)\ \chi_{23}\}}{(\gamma - 1)} - \frac{\chi_{23}}{\{1 + (\gamma-1)\chi_{23}\}} \right]$$

(4.4.3)

5   RECIRCULATION RATIO AND MOMENTUM CONSERVATION

Recirculation ratio R is derived from the momentum conservation equation, by assuming a steady state condition. Figure 5.1 below illustrates the steam separator, and the main parameters of interest.
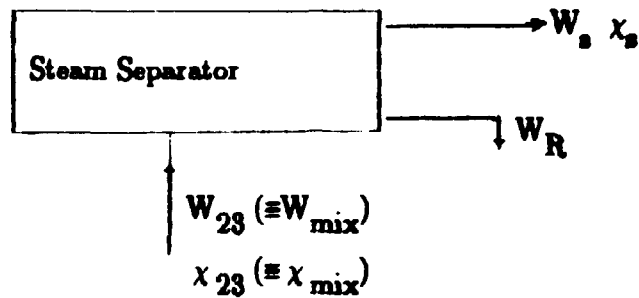

Figure 5.1 Model of Steam Separator.

5.1   Recirculation Ratio R

From Equation 2.4.14 one gets, in the tube regions, Region 1Q, 1F, 2Q and 2F,

$$\dot{Q}_T = W_{mix}\, h_{mix} - W_{51}\, h_{51} \tag{5.1.1}$$

where

$$W_{mix} = W_{f23} + W_{g23} = W_{51} \tag{5.1.2}$$

$$h_{mix} = \frac{W_{f23} h_f + W_{g23} h_g}{W_{mix}} = h_f + \frac{W_{g23}}{W_{mix}} h_{fg} \tag{5.1.3}$$

$\dot{Q}_T$ = steam generator power(steady state),

and defining the recirculation rate R as

$$R = \frac{W_{mix}}{W_s}$$

with $\chi_s W_s = W_{g23} = \chi_{mix} W_{mix}$, one gets a simple expression

$$R = \frac{\chi_s}{\chi_{mix}}$$

and the expression for the feed mixture enthalphy, 5.1.3, can be rewritten as

$$h_{mix} = h_f + \frac{\chi_s}{R} h_{fg} \quad \text{(5.1.4)}$$

Downcomer is fed by W_R and W_F, such that one can write

$$W_{51} = W_R + W_F \quad \text{(5.1.5-a)}$$

and

$$W_{51} h_{51} = W_R h_f + W_F h_F ; \quad \text{(5.1.5-b)}$$

and since a steady state condition is assumed, one gets R as

$$R = W_{51}/W_F \quad \text{(5.1.6)}$$

Combining Equations 5.1.5-a, 5.1.5-b and 5.1.6 the result is

$$R = \frac{h_f - h_F}{h_f - h_{51}} = \frac{\Delta H_F}{\Delta H_{51}} \quad \text{(5.1.7)}$$

that is, R is the ratio of the inlet subcooling to the tube region inflow subcooling.

Combining Equation 5.1.1 and 5.1.4, yields

$$\dot{Q}_T = W_{51} \left(\frac{\chi_s}{R} h_{fg} + \Delta H_{51} \right) \quad \text{(5.1.8)}$$

and by substituting ΔH_{51} from Equation 5.1.7 into Equation 5.1.8 the result is

$$R = \frac{W_{51}}{\dot{Q}_T} \left(h_{fg} \chi_s + \Delta H_F \right) \quad \text{(5.1 9)}$$

or

$$R = \frac{W_{51}}{\dot{Q}_T} \left(h_g - h_F \right), \text{ if } \chi_s = 1.0. \quad \text{(5.1.10)}$$

Therefore, the computation of R requires the value of W_{51}, which can be calculated through the momentum conservation in the recirculation loop. Weakly contributing term will be neglected, but, for the clarity, some of then will be temporarily retained in the explanation below.

5.2 Momentum Conservation

The momentum conservation equation, Equation 2.3.11, is transcribed below for the clarity.

$$\frac{1}{A_k} \frac{d}{dt} G_k(t) = \frac{W_i v_i - W_o v_o}{A_k} - \frac{\rho v^2}{2D_e} f_{DW} L_k$$

$$(P_i - P_o) + g\cos\theta(\rho_o z_o - \rho_i z_i). \tag{5.2.1}$$

where

$$G_k(t) = A_k \int_{z_i(t)}^{z_o(t)} \rho v \, dz . \tag{5.2.2}$$

f_{DW} = Darcy–Weisbach friction factor($f_F = f_{DW}/4$).

The time derivative term is negligible in the recirculation circuit except in the downcomer region where the velocity is relatively higher. Therefore the left hand side of Equation 5.2.1 will only be considered in region 5 (downcomer region).

From the definition of $G_k(t)$, assuming saturated liquid density, one can write, in region 5:

$$G_5(t) = A_5 \rho_f v_5 L_5 \tag{5.2.3}$$

such that the left hand side of Equation 5.2.1 becomes

$$\frac{d}{dt} G_5(t) = A_5 \rho_f v_5 \frac{d}{dt} L_5 + L_5 \frac{d}{dt}(A_5 \rho_f v_5) . \tag{5.2.4}$$

Recalling the definition of W_o, Equation 2.2.6, one gets

$$W_{51} = A_5 \, \rho_f \, v_5 \tag{5.2.5}$$

which inserted in Equation 5.2.4 , yields

$$\frac{d}{dt}G_5(t) = W_{51}\frac{d}{dt}L_5 + L_5\frac{d}{dt}W_{51} \, . \tag{5.2.6}$$

From Equation 3.2.7 one gets

$$\frac{d}{dt}L_5 = \frac{W_F + W_R - W_{51}}{A_5 \, \rho_f} \, . \tag{5.2.7}$$

Substituting Equation 5.2.4 and 5.2.7 into the first term on the right hand side of Equation 5.2.6 one gets

$$\frac{d}{dt}G_5(t) = (W_F + W_R - W_{51})v_5 + L_5\frac{d}{dt}W_{51} \, . \tag{5.2.8}$$

Equation 5.2.1 will be used throughout the recirculation circuit regions observing though that the time derivative term is only retained in the downcomer region. The right hand side collects the pressure loss terms in the control volumes.

Acceleration term

In region 5, the downcomer region, the dissipative pressure loss term, the first term on the right hand side of Equation 5.2.1, is canceled out by the corresponding term on the left hand side, according to Equation 5.2.8 .

In the subcooled region and in two-phase region the acceleration term is negligible, its contribution being a few cents of the total pressure loss.

In the bulk boiling regions the slip-flow model will be considered such that the inlet and outlet flow rates are given as

$$W_{i2} \, v_{i2} = W_{51} \, v_1 \tag{5.2.9-a}$$

$$W_{o2} \, v_{o2} = W_{f2} \, v_{f2} + W_{g2} \, v_{g2} \tag{5.2.9-b}$$

with

$$W_{51} = \rho_f \, v_1 \, A_2 \quad , \tag{5.2.10-a}$$

$$W_{f2} = \rho_f \, v_{f2} \, A_2 (1-\alpha_2) = (1-\chi_2) \, W_{51} \quad \text{, and} \tag{5.2.10-b}$$

$$W_{g2} = \rho_g \, v_{g2} \, A_2 \alpha_2 = \chi_2 \, W_{51} \, . \tag{5.2.10-c}$$

Substitution of the expression for v_1 from Equation 5.2.10–a in 5.2.9–a, results in

$$W_{i2} \, v_{i2} = \frac{W_{51}^2}{\rho_f \, A_2} \tag{5.2.11}$$

Combining Equations 5.2.10–a, 5.2.10–b and 5.2.10–c with Equation 5.2.9–b, one gets

$$W_{o2} \, v_{o2} = \frac{W_{51}^2}{A_2} \left[\frac{(1-\chi_2)^2}{(1-\alpha_2)} \frac{1}{\rho_f} + \frac{\chi_2^2}{\alpha_2} \frac{1}{\rho_g} \right] \tag{5.2.12}$$

Therefore, the acceleration term in the recirculation circuit can be summarised as

$$\sum_k \frac{(W_i v_i - W_o v_o)}{A_k} = -\frac{W_{51}^2}{A_2} \left[\{ \frac{(1-\chi_2)^2}{(1-\alpha_2)} - 1 \} \frac{1}{\rho_f} + \frac{\chi_2^2}{\alpha_2} \frac{1}{\rho_g} \right] . \tag{5.2.13}$$

The values of χ_2 and α_2 can be defined as

$$\alpha_2 = (\alpha_{2Q} + \alpha_{2F})/2$$

and

$$\chi_2 = (\chi_{2Q} + \chi_{2F})/2 \, .$$

Gravity term

The gravity term represents the driving force for the natural circulation, against which counteract the friction and form pressure losses.

The gravity term, the last term in Equation 5.2.1, can be written in the recirculation circuit as

$$\sum_k g \cos \theta (\rho_o z_o - \rho_i z_i) = g \rho_f [L_5 - (L_1 + L_2' + L_3')] \tag{5.2.14}$$

where the approximating assumptions are

$$L_1 = (L_{1Q} + L_{1F})/2 \tag{5.2.14-a}$$

$$L_2' = (L_{2Q}' + L_{2F}')/2 \tag{5.2.14-b}$$

$$L_3' = (L_{3Q}' + L_{3F}')/2 \tag{5.2.14-c}$$

with the prime superscripts standing for the collapsed mixture height defined, for example, by

$$L_{2Q}' = \frac{\rho_{2Q}}{\rho_f} L_{2Q} ,$$

where

$$\rho_{2Q} = \alpha_{2Q} \rho_g + (1 - \alpha_{2Q}) \rho_f .$$

Friction and Form Factors

The friction force is the main resistive force against the natural circulation, and it depends on geometrical factors and flow conditions in a complex way such that its estimation is beyond the analytical capability. In both one—phase and two—phase flow the friction factor for liquid phase will be estimated by Blasius's formula,

$$f_{DW} = 0.316 \, Re^{-0.25} . \tag{5.2.15-a}$$

In two—phase flow an improved correction factor/1/ based on Martinelli—Nelson factor, ϕ_{LO}^2 , will be used. It is independent of flow for flow rates lower than $1.000 \text{kg/m}^2/\text{s}$.

According to the values tabulated in reference 1, the values of ϕ_{LO}^2 in a restricted range of pressure can be correlated as

$$\phi_{LO}^2 = (1 + 18.65\chi) \left(\frac{41.4}{P(bar)} \right)^b \qquad (5.2.15\text{-}b)$$

where

$$b = \begin{bmatrix} 1.14 & \text{for } \chi \geq 0.30 \\ 0.375(\ln\chi + 4.605)^{0.9} & \text{for } 0 < \chi < 0.30 \end{bmatrix}$$

$$P \simeq (30 - 60) \text{ bar }.$$

The sum of friction pressure loss terms in region 5, 1 and 2 can be written as

$$\sum_{k=1,2,5} \frac{-\rho v^2}{2D_e} f_{DW} L_k = \frac{-W_{51}^2}{2\rho_f A_2^2} \left[\frac{f_{DW5} L_5 A_2^2}{D_{e5} A_5^2} + \frac{f_{DW1} L_1}{D_{e1}} + \frac{f_{DW2} L_2 \phi_{LO}^2}{D_{e2}} \right] . \qquad (5.2.16)$$

In the separator region the pressure loss is a resultant of complex phenomena, involving contraction, as much as acceleration, friction and expansion, such that practical correlations based on experiments are of upmost necessity. But as a first approximation the pressure loss in the separator can be assumed to be proportional to the square of the flow rate.

The constant of proportionality can be adjusted provisionally by setting the downcomer liquid level at the nominal water level.

Thus, the friction loss term in the separator can be written as

$$\Delta P_{separator} = - K_3 \frac{W_{51}^2}{2\rho_f A_3^2} . \qquad (5.2.17)$$

The flow restrictor in the downcomer has a variable form factor depending upon its position in the flow channel. Thus, analogously to the separator form factor, the restrictor form factor will be set by adjusting the downcomer liquid level at the desired level. The pressure loss at the restrictor will be given as

$$\Delta P_{restrictor} = -K_5 \frac{W_{51}^2}{2\rho_f A_5^2}.$$ (6.2.18)

During the expansions the pressure variation, both for one–phase and two–phase, will be estimated as

$$\Delta P_{1\phi_e} = (\frac{A_1}{A_2} - \frac{A_1^2}{A_2^2}) \frac{W^2}{\rho_f A_1^2}$$ (6.2.19–a)

$$\Delta P_{2\phi_e} = (\frac{A_1}{A_2} - \frac{A_1^2}{A_2^2}) \frac{W^2}{A_1^2} \left[\frac{(1-\chi)^2}{(1-\alpha)} \frac{1}{\rho_f} + \frac{\chi^2}{\alpha} \frac{1}{\rho_f} \right]$$ (6.2.19–b)

and during the contractions the loss terms will be given as

$$\Delta P_{1\phi_e} = \frac{(1 + a)}{2} (1 - \frac{A_1^2}{A_2^2}) \frac{W^2}{\rho_f A_1^2}, \quad a \simeq 0.4,$$ (6.2.20–a)

$$\Delta P_{2\phi_e} = \frac{(1 + a)}{2} (1 - \frac{A_1^2}{A_2^2}) \frac{W^2}{\rho_f A_1^2} \frac{(1-\chi)^2}{(1-\alpha)}, \quad a \simeq 0.2.$$ (6.2.20–b)

During the expansion and contraction, in two–phase flow, the void fraction α is assumed as a constant before and after an expansion(contraction). Therefore no phase change is admitted during the flow passage from one area to another.

One can notice larger pressure losses at the following particular locations:

- restrictor , $K \approx 19$,
- tube support, $K \approx 7.5$/each,
- vapor separator, $K \approx 18$.

Therefore the minute contributions such as arising from the acceleration and localised expansion/contraction terms will be neglected term by term as long as numerical estimative corroborate its degree of insignificance.

However, considering that the pressure loss in the separator includes the effects of the contraction and expansion, Equation 5.2.6 becomes, recalling Equation 5.2.13, 5.2.14, 5.2.16, 5.2.17 and 5.2.18,

$$
\frac{L_5}{A_5}\frac{d}{dt}W_{51} = -\frac{W_{51}^2}{A_2^2}\left[\left\{\frac{(1-\chi_2)^2}{(1-\alpha_2)} - 1\right\}\frac{1}{\rho_f} + \frac{\chi^2}{\alpha}\frac{1}{\rho_g}\right]
$$

$$
+ g\rho_f[L_5 - (L_1 + L_2' + L_3')]
$$

$$
\frac{-W_{51}^2}{2\rho_f A_2^2}\left[\frac{f_{DW5}L_5 A_2^2}{D_{e5} A_5^2} + \frac{f_{DW1}L_1}{D_{e1}} + \frac{f_{DW2}L_2\phi_{LO}^2}{D_{e2}}\right]
$$

$$
- K_3\frac{W_{51}^2}{2\rho_f A_3} - K_5\frac{W_{51}^2}{2\rho_f A_5} \qquad (5.2.21)
$$

Since $A_2 = A_1$, the equation above can be rearranged, in terms of momentum of region 1, as

$$
\frac{L_5}{A_5}\frac{d}{dt}W_{51} = g\rho_f[L_5 - (L_1 + L_2' + L_3')]
$$

$$
- \frac{W_{51}^2}{2\rho_f A_1^2}\left[2\left\{\frac{(1-\chi_2)^2}{(1-\alpha_2)} - 1 + \frac{\chi^2}{\alpha_2}\frac{\rho_f}{\rho_g}\right\} + \frac{f_{DW1}L_1}{D_{e1}}\right.
$$

$$
\left. + \frac{f_{DW2}L_2\phi_{LO}^2}{D_{e2}} + \left(\frac{A_1}{A_5}\right)^2\left(\frac{f_{DW5}L_5}{D_{e5}} + K_5\right) + \left(\frac{A_1}{A_3}\right)^2 K_3\right]
$$

$$
(5.2.22)
$$

Among several approximations, one can cite the pressure loss estimation in the tube supports, which are estimated to be of the order of

$$
\Delta P_{suport1} = K_{suport1}\frac{W_{51}^2}{2\rho A_1^2} ,
$$

with $K_{suport1} \simeq 7.5$;

in addition to the restrictor form factor which is relatively high, $K \simeq 18.7$.

Equation 5.2.22 is approximated in GVTRAN-PC by neglecting the left hand side term since its contribution has found to be about four order of magnitude smaller than the rest of the terms in a pump trip transient.

On the other hand its inclusion in the program had only been made possible with the use of very small integration time-steps, order of 0.0001 second in the classical Runge-Kutta scheme, the restriction being the numerical stability criteria.

Without the time derivative term the integration time-step can be as large as 0.05 second, allowing a significant computational load reduction while the degree of accuracy of the complete model is practically retained.

7. DEFINITION OF THE CORRELATIONS

The heat transfer coefficients are presented in the next paragraphs, but wherever applicable they are treated as constant parameters with the objective of alleviating the computational burden.

One-phase Flow

The one-phase transfer coefficient is estimated, in the turbulent flow regimen($Re > 3.000$), with Dittus-Boelter,

$$h_{DB} = 0.023 \frac{k}{D_e} Re^{0.8} Pr^n \quad (W/m^2/^\circ C) \qquad (7.1)$$

where

n = 0.4 in secondary side and 0.3 in primary side,

k = fluid thermal conductivity($W/m/^\circ C$),

D_e = inner diameter(primary side)

or equivalent diameter(secondary side) (m).

The temperature during a transient experiences variation in the range of $20^\circ C$ and the pressures vary not more than 15bar, resulting, therefore, in small variations in k, ρ, c_p and μ, such that the convection coefficient could primarily be determined by the fluid velocity. Thus an expression for h can succinctly be written, in the neighborhood of the operation condition, as

$$h_{DB} = constant\ W^{0.8} . \qquad (7.2)$$

Two-phase flow

Thom's correlation in two-phase turbulent flow is given, for pressures ranging between 750 and 2000psia, as

$$(T_w - T_{sat}) = 0.072(q'')^{0.5}/\ exp(P/1260) \qquad (7.3)$$

where

T_w = wall temperature ($^\circ F$),

T_{sat} = saturation temperature ($^\circ F$),

q'' = heat flux (Btu/hr/ft^2),

P = pressure (psia).

Therefore the convective heat transfer coefficient in two-phase turbulent flow can be expressed as

$$h_{Thom} = 1973 \, (T_w - T_{sat}) \, \exp(P/43.5) \; (W/m^2/{}^{\circ}C) \qquad (7.4)$$

where T_w and T_{sat} are in ${}^{\circ}C$, and P in bar.

Local Boiling Regimen

Whereas not treated in GVTRAN-PC program, the transition region between the subcooled flow and bulk boiling flow can be correlated for pressures in 500-2000 psia range with Jens-Lottes. It is also valid for low-quality saturated flows:

$$(T_w - T_{sat}) = 60 \, (q''/10^6)^{0.25}/ \exp(P/900) \qquad (7.5)$$

with

T_w and T_{sat} in ${}^{\circ}F$,

q'' in $Btu/hr/ft^2$, and
P in psia.

The convective heat transfer coefficient can therefore be correlated with

$$h_{JL} = 2556 \, (T_w - T_{sat})^3 \, \exp(P/15.5) \; (W/m^2/{}^{\circ}C) \qquad (7.6)$$

where

T_w and T_{sat} are in ${}^{\circ}C$ and P in bar.

In the GVTRAN-PC program the two-phase flow region will be assumed to begin at the point where the saturation temperature is reached. At this point the void fraction and quality will be assumed to be zero.

8. IMPROVED DOWNCOMER MODEL

It is known, by experience, that a correct modelling of the downcomer as well as a correct prediction of the subcooled fluid density is of the prime importance for an accurate estimation of the feed chamber water level.

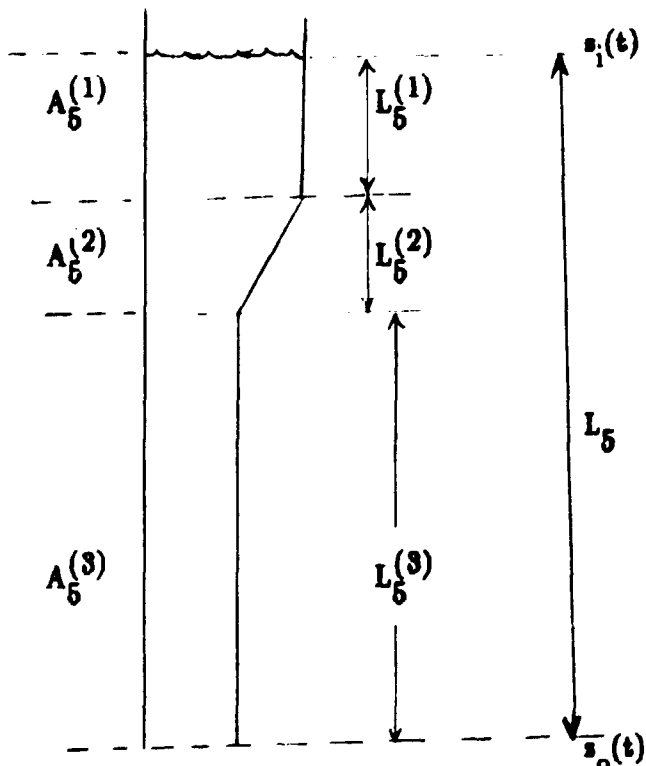Figure 8.1 below illustrates the downcomer flow channel model defined in GVTRAN–PC program.

Figure 8.1 Model of improved downcomer in GVTRAN–PC.

The flow area $A_5^{(2)}$ is the average flow area, and the area $A_5^{(1)}$ and $A_5^{(3)}$ are considered as constants.

The average flow area in L_5 , $\overline{A}_5$, can be defined as

$$\overline{A}_5 = \frac{1}{L_5}(L_5^{(1)}A_5^{(1)} + L_5^{(2)}A_5^{(2)} + L_5^{(3)}A_5^{(3)})$$ (8.1-a)

where $\qquad L_5 = L_5^{(1)} + L_5^{(2)} + L_5^{(3)}$ (8.1-b)

Therefore, the following equalities are obtained:

$$\frac{d}{dt}(\overline{A}_5 L_5) = A_5^{(1)}\frac{d}{dt}L_5^{(1)}$$ (8.1-c)

and

$$\frac{d}{dt}L_5^{(1)} = \frac{d}{dt}L_5$$ (8.1-d)

Mass Conservation

The mass conservation equation, Equation 2.2.7, can be rewritten as

$$\frac{d}{dt}\overline{\rho}_k = \frac{W_i - W_o - \overline{\rho}_k\frac{d}{dt}(\overline{A}_k L_k)}{\overline{A}_k L_k}$$ (8.2)

Considering the slow variation of the density in time, one can neglect the left hand side of Equation 8.2, yielding

$$\rho_5\frac{d}{dt}(\overline{A}_5 L_5) = W_F + W_R - W_{51}$$ (8.3)

Making use of Equation 8.1-c and 8.1-d, one can rewrite Equation 8.3 as

$$\frac{d}{dt}L_5 = (W_F + W_R - W_{51})/(\rho_f A_5^{(1)})$$ (8.4)

This equation must replace Equation 3.2.7 in the variable flow area downcomer model.

Energy Conservation

The energy conservation equation, Equation 3.3.27, in the variable flow area downcomer model can be rewritten as

$$\frac{d}{dt}(\rho_f h_f \overline{A}_5 L_5) = W_F h_F + W_R h_f - W_{51} h_{51} \cdot \quad (8.5)$$

By utilising the expression for the derivative of L_5 , Equation 8.4, the above equation becomes, with the help of Equation 8.1–c and 8.1–d,

$$\frac{d}{dt}h_5 = [W_F h_F + W_R h_f - W_{51} h_{51}$$

$$- h_5(W_F + W_R - W_{51})]/(\rho_f \overline{A}_5 L_5). \quad (8.6)$$

This equation must substitute Equation 3.3.28 and 3.3.29, in the variable flow area downcomer model.

Momentum Conservation

The momentum conservation equation, Equation 5.2.1, will present some modifications in the variable flow area downcomer model.

Equation 5.2.3 is rewritten as

$$G_5 = \rho_f \left(v_5^{(1)} L_5^{(1)} A_5^{(1)} + v_5^{(2)} L_5^{(2)} A_5^{(2)} + v_5^{(3)} L_5^{(3)} A_5^{(3)} \right) \quad (8.7)$$

and considering the mass flux continuity and Equation 8.1–d, one gets

$$\frac{d}{dt}G_5 = L_5 \frac{d}{dt}W_{51} + W_{51}\frac{d}{dt}L_5 \cdot \quad (8.8)$$

Substituting the derivative of L_5 , Equation 8.4, Equation 8.8 results in

$$\frac{d}{dt}G_5 = L_5 \frac{d}{dt}W_{51} + (W_F + W_R - W_{51})W_{51}/(\rho_f A_5^{(1)}) \cdot \quad (8.9)$$

The acceleration term in the downcomer, i.e., the first term on the right hand side of Equation 5.2.1, is written as

$$\Delta P_{acel} = \frac{W_i v_i - W_o v_o}{\overline{A}_k} , \quad (8.10)$$

where it is noticed that A_k has been replaced by $\overline{A}_k$.

Since in volume 5 both v_i and v_o are

$$v_i = v_5^{(1)} \qquad \text{and} \qquad v_o = v_5^{(3)},$$

one can express the term ΔP_{acel} as

$$\Delta P_{acel} = \frac{(W_F + W_R)v_5^{(1)} - W_{51}v_5^{(3)}}{\overline{A}_5} \tag{8.11}$$

From the definition of mass flux the expressions

$$v_5^{(3)} = \frac{W_{51}}{\rho_f A_5^{(3)}} \qquad \text{and} \qquad v_5^{(1)} = \frac{W_{51}}{\rho_f A_5^{(1)}}$$

are obtained, which inserted in Equation 8.11, yields

$$\Delta P_{acel} = \frac{W_{51}}{\rho_f A_5^{(1)} \overline{A}_5} \left(W_F + W_R - W_{51} \frac{A_5^{(1)}}{A_5^{(3)}}\right). \tag{8.12}$$

Thus, the second term on the left hand side of Equation 8.9 divided by $\overline{A}_5$ was not completely canceled out as had been in the case of constant flow area downcomer model.

The resultant on the right hand side is given as

$$\Delta P_{acel} = \frac{- W_{51}^2}{\rho_f A_5^{(1)} \overline{A}_5 A_5^{(3)}} \left(\frac{A_5^{(1)}}{A_5^{(3)}} - 1\right). \tag{8.13}$$

Therefore, this term must be added to the right hand side of Equation 5.2.13, and to the right hand side of Equation 5.2.21 and 5.2.22.

The friction loss term in region 5 can be partitioned in three terms as

$$\frac{f_{DW5}}{D_{e5}} \frac{L_5}{A_5^2} \frac{A_2^2}{A_5^2} = \sum_{i=1}^{3} \frac{f_{DW5}^{(i)}}{D_{e5}^{(i)}} \frac{L_5^{(i)} A_2^2}{A_5^{(i)2}} \qquad (8.14)$$

In the practice, however, the insignificant terms of Equation 5.2.22 will be neglected.

In general, the largest contribution to the form factor is the one due to the restrictor, and the most important friction loss term comes from region $V_5^{(3)}$

9. NUMERICAL ALGORITHM

The simplicity being one of the desired characteristics in GVTRAN–PC program, the cross flow in the secondary side of the steam generator was disregarded. Hence one control volume for subcooled region and one control volume for bulk boiling region were defined. Under this simplified configuration the new notations will be

— subscript 1 for the subcooled region and
— subscript 2 for the bulk boiling region.

In the steady state condition the mass conservation equation yields

$$W_{51} = W_{12} = W_{23} \quad ,$$

$$W_{23} = W_{s} + W_{R} \quad ,$$

$$W_{R} + W_{F} = W_{51} \quad ,$$

$$W_{34} = W_{23} - W_{R} \quad \text{and}$$

$$W_{F} = W_{s} \quad .$$

From the energy conservation equation, Equation 3.3.27,

$$W_{F}h_{F} + W_{R}h_{f} = W_{51}h_{51}$$

and since $\quad R = \dfrac{W_{51}}{W_{F}} = \dfrac{\Delta H_{F}}{\Delta H_{51}}$

one gets $\quad R = \dfrac{W_{51}}{\dot{Q}_{T}}(h_{fg} + \Delta H_{F})$

from which one can deduce the value of W_{51} , for the known values of R, $\dot{Q}_{T}$ and ΔH_{F} .

But since

$$W_{R} = W_{51} - W_{F} \quad ,$$

it results, from Equation 3.3.27,

$$h_{51} = \frac{W_F h_F + (W_{51} - W_F) h_f}{W_{51}}$$

or

$$h_{51} = h_f - (h_f - h_F)/R \quad ,$$

and, from Equation 3.3.3,

$$W_{51}(h_{51} - h_f) = -S_1 q''$$

where $S_1 = L_1 M_1$, resulting in

$$L_1 \frac{W_{51}(h_f - h_{51})}{M_1 q''} \quad .$$

From Equation 3.3.6 one gets

$$W_{51}(h_{23} - h_f) = M_2(L - L_1)$$

hence

$$h_{23} = h_f + \frac{M_2}{W_{51}} (L - L_1) q_2''$$

and its value can be utilized in the computation of χ_{23} and α_{23} .

Alternatively, Equation 3.3.15 can be used to get

$$h_{23} = h_f + \frac{\chi_s}{R} h_{fg} \quad .$$

Equation 3.3.18 yields

$$L_3 = \frac{V_L}{(1 - \alpha_3) A_3}$$

and the mixture level, L_3 , must be given as a boundary condition.

Equation 5.2.22 gives the relationship of momentum conservation in the steady state condition

$$g\rho_f[L_5 - (L_1 + L_2' + L_3')] = \frac{W_{51}^2}{2\rho_f A_1^2} \text{ function}(a, \chi, f_{DW}, K_1, K_2, K_3, K_5).$$

This relationship is utilised in an iterative manner during the form factor search.

ITERATIVE ALGORITHM

The steady state condition is obtained by searching for the parameters, in an iterative scheme, until the input boundary conditions has been satisfied.

The boundary conditions at the steady state are:

- Secondary: χ_s, h_F, W_F, P_s, R, L_5, L_3 and Power.

- Primary: P, T_{prim} and W.

The iterative algorithm is described as:

1) Determine the values of W_{51} and χ_{23}, with

$$R = \frac{W_{51}}{W_F} = \frac{\chi_s}{\chi_{23}},$$

2) Calculate h_{51} with the expression

$$h_{51} = h_f - (h_f - h_F)/R,$$

3) Calculate L_1, for primary and secondary, with

$$L_1 = \frac{W_{51}}{M_1 q_1''} (h_f - h_{51})$$

where
q_1'' is obtained with Dittus–Boelter,

4) Calculate h_{23}', therefore χ_{23}', as

$$h'_{23} = h_f + \frac{q_2^n M_2 L_2}{W_{51}}$$

where
q_2^n is obtained with Dittus–Boelter and Thom.

5) Compare χ'_{23} to χ_{23} from step 1, and obtain the correction factor

$$F_{correction} = \frac{\chi_{23}}{\chi'_{23}}$$

6) Multiply h_{Thom} by $F_{correção}$, and go to step 4.

After the convergence in χ_{23} , the momentum iteration is performed in order to adjust the form factor values:

$$K_1, K_2, K_3, K_5$$

isolately, or any set of them at the same time.

10. GVTRAN–PC TEST CALCULATIONS

GVTRAN program was tested against the actual transient measurements recorded during a startup testing of Donald C. Cook Nuclear Station Unit One ("Supplement to Donald C. Cook Nuclear Plant Unit One Startup Report", Indiana and Michigan Power Company(September 1976)). The transient consisted of a plant turbine trip from 100% of the rated power. The boundary conditions for the initial steady state calculation is given in Table 10.1 .

TABLE 10.1

Initial Steady State Boundary Conditions
for D.C. Cook turbine trip transient.

Mass flow rate(lbm/hr)	
primary inlet	3.67×10^7
feed inlet/steam outlet	3.3×10^6
Pressure (psia)	
primary inlet	2240
steam dome	738
Temperature (°F)	
primary inlet	594
feed inlet	435
Feed chamber water level (ft)	8.5
Recirculation ratio	3.25

The turbine trip was manually initiated while the plant was operating at full power. Thereafter the main steam turbine stop valve was automatically closed causing, as a consequence, the trip of the reactor and turbine driven feed pumps. The boundary conditions for GVTRAN–PC input are

      – in the secondary side: the steam outlet mass flow rate and feed inlet mass flow rate and temperature;

      – in the primary side: the inlet pressure, temperature and mass flow rate.

The steam flow rate after the turbine trip is shown in Figure 10.1. The sudden drop in the flow rate caused by the stop valve closure is followed by a reduced flow rate through the relief valve during few additional seconds.

The feedwater flow rate is shown in Figure 10.1 and Figure 10.2 presents the primary coolant temperature.
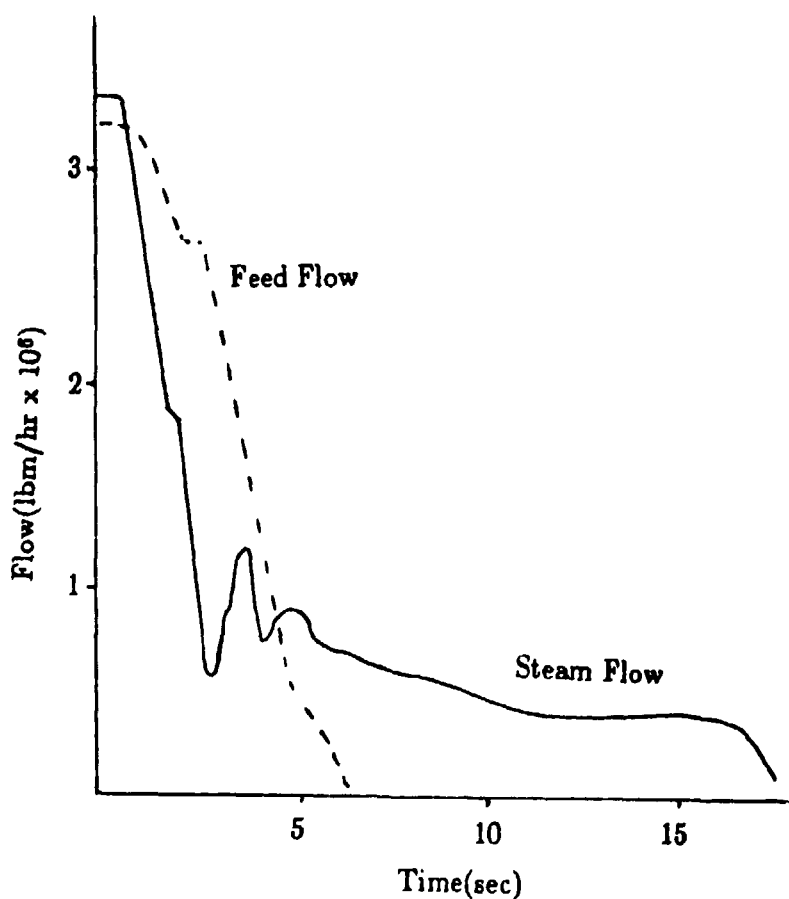

Figure 10.1 — Steam and feedwater flow rate for D.C. Cook turbine trip transient.
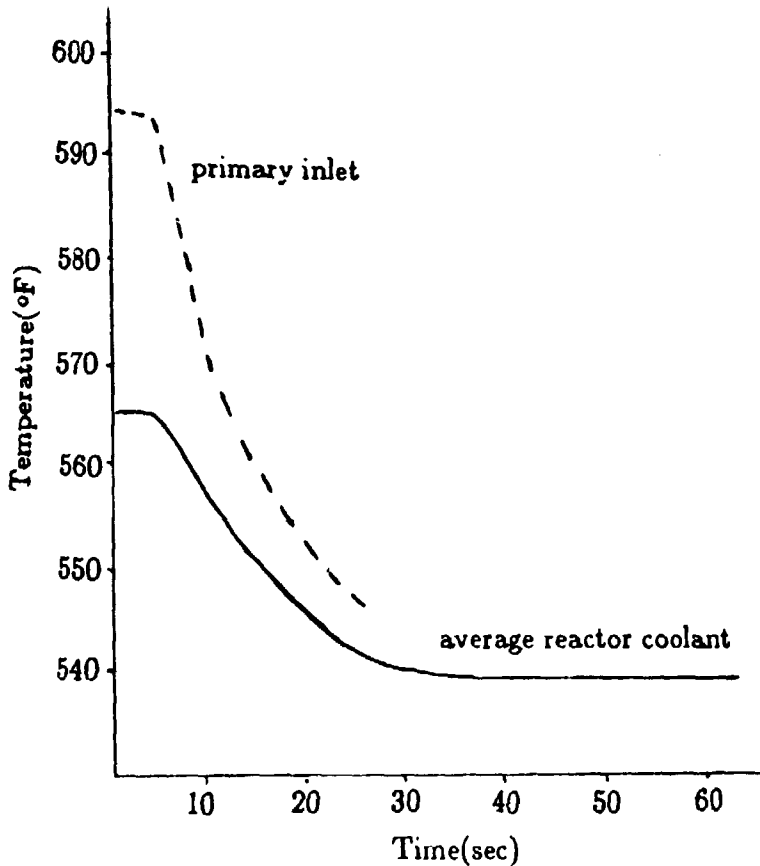
Figure 10.2 – Primary coolant temperature for D.C. Cook turbine trip transient.

The feed chamber water level and the steam dome pressure calculated with GVTRAN–PC program is plotted in Figure 10.3 and 10.4 together with the experimental data and results calculated with the TRANSG/4/ program. The comparison of the results is quite satisfactory in spite of the simplified model employed in GVTRAN–PC program in comparison with the TRANSG 4—equation drift—flux model. Both water level and pressure deviations are well within the acceptable range considering the margin of uncertainties in the experimental data.

The computational expenditures was not directly compared, but a partial prognostic can be inferred from the smaller number of conservation equations and control volumes which are required in the GVTRAN–PC program, viz. 4 control volumes in primary side and 4 control volumes in the secondary side, against 18 and 16 control volumes, respectively, in TRANSG program.
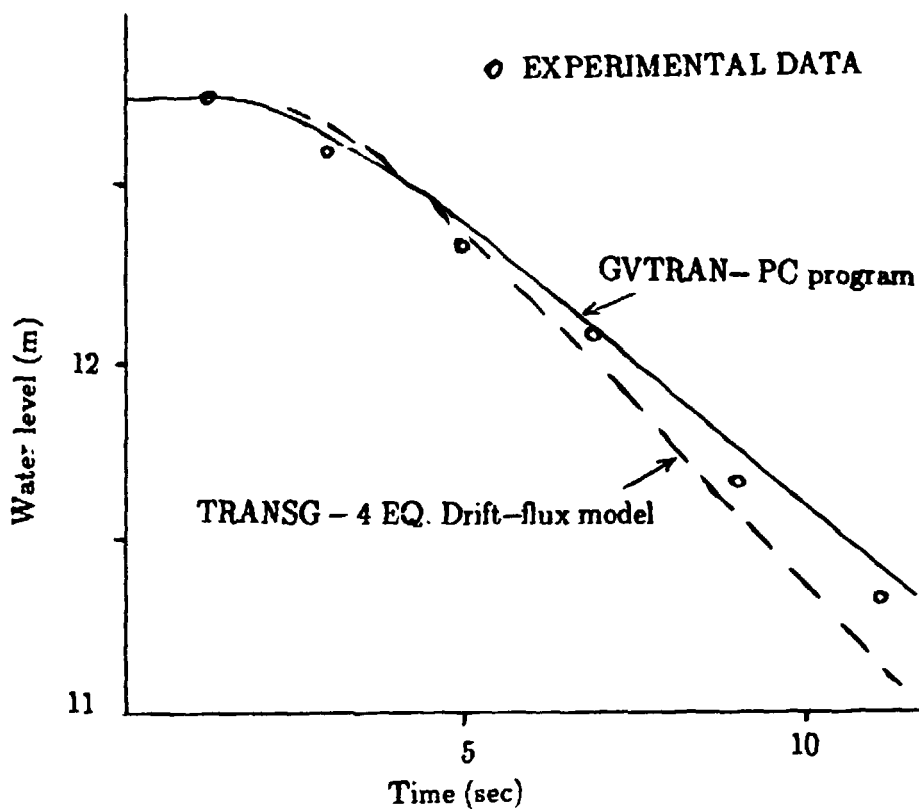
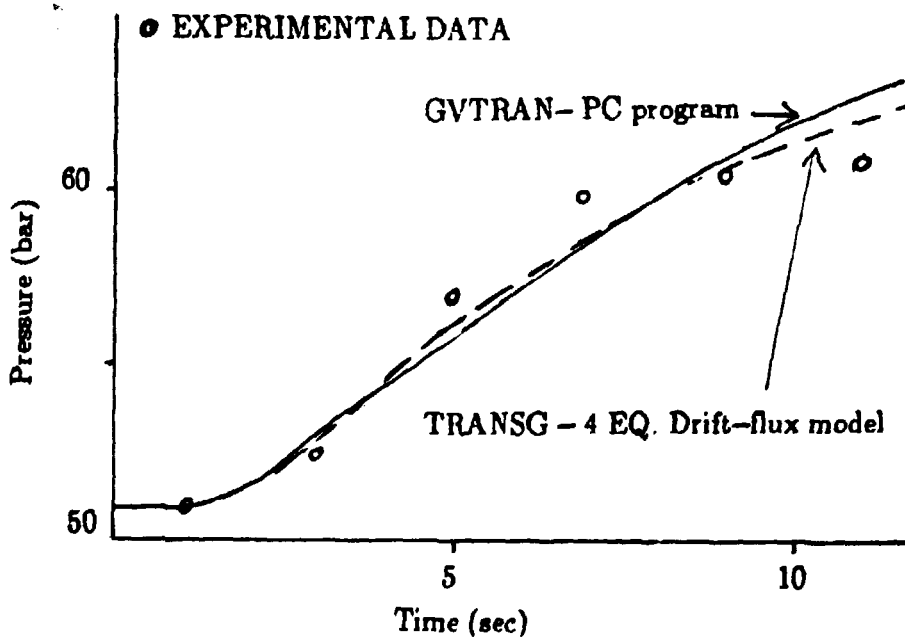Figure 10.3 — Feed chamber water level in D.C. Cook transient.

Figure 10.4 — Steam chamber pressure in D.C. Cook transient.

11.   CONCLUDING REMARKS

The steam generator model presently developed and implemented in GVTRAN–PC program has been demonstrated to be satisfactorily accurate in reproducing a typical transient in a PWR nuclear station.

The accuracy of the results was not compromised even with the use of the fewer control volumes, only two volumes in the secondary tube region, because the moving boundary approach had been adopted at the boundary of the bulk boiling region, permitting, thus, a fairly good representation of the time variation of the two–phase region height without the recourse to a fine mesh representation.

The momentum conservation equation has only been balanced in the secondary region, and its solution by a quasi–static approach resulted in a significant saving in the computation time, whereas retaining a good accuracy in the water level representation.

In conclusion, GVTRAN–PC possess a combination of few characteristics, all of them highly praised in a nuclear plant simulator: coding simplicity for a quick intermachine transfer, computation velocity compatible with on–line monitoring, and accuracy acceptable for a typical transient analysis.

12. REFERENCES

1. THOM, J.R.S. Prediction of pressure drop during forced circulation boiling of water, Int. J. Heat Mass Transfer, 7:709, 1964.

2. BIRD, R.B.; STEWART, W.E.; LIGHTFOOT, E.N. Transport Phenomena. New York, John Wiley, 1960.

3. TONG, L.S. Boiling heat transfer and two-phase flow. New York, R.E. Krieger, 1975.

4. LEE,J.C.; AKCASU,A.Z.; DUDERSTADT,J.J.; VAN TUYLE,G.J.; FORTINO,R. Simplified models for transient analysis of nuclear steam generators. Palo Alto, CA, Electric Power Research Institute, April 1981. (EPRI NP-1772).